Project Final Report

Deposition Modeling in Support of the Michigan Mercury TMDL

USEPA Great Lakes Restoration Initiative

Grant Number GL-00E00605

Frank J. Marsik, PhD (Principal Investigator)

Sandy Sillman, PhD (Co-Investigator)

J. Timothy Dvonch, PhD (Co-Investigator)

James Barres (Quality Assurance)

Gavin Chensue (Research Assistant)

Zachary Ebenstein (Research Assistant)

Original Submission: February 18, 2014

Revised Submission: June 26, 2014

Table of Contents

LIST OF FIGURES 3

LIST OF TABLES 5

LIST OF SELECTED ABBREVIATIONS 6

Executive Summary 7

I. Meteorological Simulations 10

Methodology 10

Pre-simulation Sensitivity Evaluations 12

WRF-Simulation Evaluations 17

II. Emissions Processing 25

Methodology – Raw Emissions Input Files 25

Methodology – Creation of CMAQ "Model-Ready" Emissions Files 26

Emissions Processing Results 28

III. CMAQ Regional Chemistry Simulations 29

Methodology 29

CMAQ MODEL BASE CASE Simulation Results 44

CMAQ Model REDUCED EMISSIONS SCENARIO Estimates 53

CMAQ Model REDUCED EMISSIONS SCENARIO Estimates (Statewide Totals) 54

IV. Conclusions 55

V. Acknowledgements 57

LIST OF FIGURES

Figure 1. WRF modeling domain utilizing three nested domains: 36-km (CONUS), 12-km (northeastern US) and 04-km (Great Lakes watershed). 11

Figure 2. Comparison of modeled and measured precipitation for select locations within 4km modeling grid for Calendar Year 2005 WRF BASE CASE simulation. 21

Figure 3. Model day-by-day wet deposition of mercury (μg/m^2) at Detroit (X's) and Grand Rapids (red squares) for (a) January and (b) July, comparing the direct deposition in the model for each day with the equivalent sum of deposition of model tagged species (conservation of mass test).....38

Figure 4. Model day-by-day dry deposition of mercury (μg/m^2) at Detroit (X's) and Grand Rapids (red squares) for (a) January and (b) July, comparing the direct deposition in the model for each day with the equivalent sum of deposition of model tagged species (conservation of mass test). 39

Figure 5. Model reduction in wet deposition of mercury (μg/m^2) at Detroit (X's) and Grand Rapids (red squares) for (a) January and (b) July, resulting from a 90 percent reduction of emissions from coal-fired power plants in the State of Michigan. The plot compares the day-by-day reduction in deposition determined as the difference between model base case and reduced emissions scenarios (horizontal axis) with the reduction derived from model tags in the base case (vertical axis). 40

Figure 6. Model reduction in wet deposition of mercury as a fraction of total mercury wet deposition at Detroit (X's) and Grand Rapids (red squares) for (a) January and (b) July, resulting from a 90 percent reduction of emissions from coal-fired power plants in the State of Michigan. The plot compares the day-by-day reduction in deposition determined as the difference between model base case and reduced emissions scenarios (horizontal axis) with the reduction derived from model tags in the base case (vertical axis). 41

Figure 7. Model reduction in dry deposition of mercury (μg/m^2) at Detroit (X's) and Grand Rapids (red squares) for (a) January and (b) July, resulting from a 90 percent reduction of emissions from coal-fired power plants in the State of Michigan. The plot compares the day-by-day reduction in deposition determined as the difference between model base case and reduced emissions scenarios (horizontal axis) with the reduction derived from model tags in the base case (vertical axis). 42

Figure 8. Model reduction in dry deposition of mercury as a fraction of total mercury wet deposition at Detroit (X's) and Grand Rapids (red squares) for (a) January and (b) July, resulting from a 90 percent reduction of emissions from coal-fired power plants in the State of Michigan. The plot compares the day-by-day reduction in deposition determined as the difference

between model base case and reduced emissions scenarios (horizontal axis) with the reduction derived from model tags in the base case (vertical axis). 43

Figure 9. Summed annual (2005) CMAQ Model BASE CASE simulation Mercury Wet- and Dry-deposition (μg/m^2) at a select series of locations across the State of Michigan. 44

Figure 10. Summed annual (2005) Total Mercury (Wet- + Dry-deposition (μg/m^2)) from 2005 CMAQ Model BASE CASE and 2001 REMSAD simulations at a select series of locations across the State of Michigan. 45

Figure 11. Comparison of mercury wet-deposition measured by the Michigan Mercury Network and mercury wet-deposition predicted by the CMAQ Model BASE CASE simulation. Each represents the annual total for Calendar Year 2005. 47

Figure 12. Calendar Year 2005 CMAQ Model BASE CASE simulation Mercury Wet- and Dry-deposition (μg/m^2) at Detroit (Livernois), MI for tagged emissions categories.....48

Figure 13. Calendar Year 2005 CMAQ Model BASE CASE Mercury Wet- and Dry-deposition (μg/m^2) at Dexter, MI field for tagged emissions categories. 49

Figure 14. Calendar Year 2005 CMAQ Hg Wet- and Dry-deposition (μg/m^2) at Grand Rapids, MI for tagged emissions categories. 50

Figure 15. Calendar Year 2005 CMAQ Hg Wet- and Dry-deposition (μg/m^2) at Flint, MI for tagged emissions categories.....51

Figure 16. Calendar Year 2005 CMAQ Model BASE CASE simulation Mercury Wet- and Dry-deposition (μg/m^2) at Pellston, MI for tagged emissions categories. 52

Figure 17. Calendar Year 2005 CMAQ Model BASE CASE Mercury Wet- and Dry-deposition (μg/m^2) at Eagle Harbor, MI for tagged emissions categories. 53

LIST OF TABLES

Table 1. WRF model parameterization options used for Michigan TMDL Study 12

Table 2. Results of METv3.0 MODE Precipitation Analysis for Cumulus Parameterization Sensitivity Analysis 13

Table 3. WRF model parameterization options using NARR model initial and boundary conditions. 14

Table 4. WRF model parameterization evaluation results.....15

Table 5. Evaluation criteria and levels of acceptance for WRF model output results.....18

Table 6. MSLP Spatial Analysis. Distances measured in kilometers, pressure measured in millibars. 19

Table 7. Results of METv3.0 MODE Precipitation Analysis for 2005 WRF BASE CASE Simulations 20

Table 8. Values given are Pierson Correlation coefficients, with highlighted cells indicating r>0.5 evaluation criteria not met.....23

Table 9. Mean Absolute Error for 00Z and 12Z Model/Observation Comparisons for the 12km Domain 24

Table 10. Comparison of total mercury emissions (by sector) between the SMOKE MODEL BASE CASE simulation and the 2005 Michigan DEQ Mercury Emissions Inventory (MDEQ 2011).....29

Table 11. Modeled emissions from Michigan and surrounding states from CMAQ Model BASE CASE simulation. 29

Table 12. Boundary condition values for the 36km Grid of our CMAQ MODEL BASE CASE simulation are given for model sigma altitudes 0.99, 0.95, 0.88, 0.72, 0.45, and 0.15, corresponding approximately to 990, 950, 880, 720, 450 and 150 hPa (millibars), respectively, for a column of air at sea level. All species not included in the table have boundary values equal to zero.....32

Table 13. Modeled emissions from Michigan and surrounding states from CMAQ Model BASE CASE simulation. 55

LIST OF SELECTED ABBREVIATIONS

The following is a list of abbreviations that were used in the body of this report. While defined within the body of the report, these abbreviations are summarized here for the convenience of the reader.

BEIS	Biogenic Emissions Inventory System
CMAQ	Community Multi-scale Air Quality
GEM	Gaseous Elemental Mercury
GOM	Gaseous Oxidized Mercury
MCIP	Meteorology-Chemistry Interface Processor
MDEQ	Michigan Department of Environmental Quality
NAM	North American Mesoscale
NARR	North American Regional Reanalysis
NEI	National Emissions Inventory
PBM	Particle Bound Mercury
PI	Principal Investigator
QA	Quality Assurance
SMOKE	Sparse Matrix Operator Kernel Emissions
TMDL	Total Maximum Daily Load
USEPA	United States Environmental Protection Agency
UTC	University Time Coordinated
WRF	Weather Research and Forecasting

Executive Summary

Having both natural and anthropogenic sources, atmospheric mercury is found primarily in the form of gaseous elemental mercury (GEM, at least 95 percent), with gaseous oxidized mercury (GOM) and particle bound mercury (PBM) present in significantly smaller amounts (Schroeder and Munthe, 1998). Exposure to mercury (primarily as methylmercury) has been linked to adverse health effects in humans (eg., Rowland *et al*., 1994; Sakamoto *et al*., 2001; Cave *et al*., 2010), as well as wildlife (e.g., Montiero *et al*., 1996; Thompson et al., 1998). As a result, over the past two decades a great deal of attention has been directed toward the development of a more complete understanding of the global environmental cycling of mercury within terrestrial and aquatic ecosystems (e.g., Amyot *et al*., 1997; Grigal, 2003; Lahoutifard *et al*., 2005; Engle *et al*., 2008).

The Clean Water Act (CWA) requires states to provide the U.S. Environmental Protection Agency (USEPA) with assessments of the quality of their waters [Section 305(b)] and a list of the waters that do not support their designated uses or do not attain set water quality standards. For waters not meeting the standard for a given contaminant, the states are required to develop estimates of total maximum daily load (TMDL) [Section 303(d)] of the contaminant to the target waters. The TMDL represents the maximum allowable loading of the contaminant in question to the target waters that will still allow the set water quality standards to be achieved.

The State of Michigan's allowable fish tissue mercury value has been set at 0.35 mg/kg. This value is the concentration that is not expected to pose a health concern to people consuming 15 grams or less of fish per day (Michigan Department of Environmental Quality [MDEQ], 2012]). Unfortunately, the MDEQ notes that there is a statewide problem with the exceedance of this standard for waters within the State of Michigan. Given that the atmosphere is believed to be the dominant source of mercury to these waters, it was determined that there was a need for a state-wide mercury TMDL to address this issue.

This project was funded by the Great Lakes Restoration Initiative (GLRI) to provide the MDEQ with estimates of the spatial distribution of total mercury deposition (both wet- and dry-) to the State of Michigan and surrounding states. Additionally, this study was to estimate how that spatial distribution might change under a reduced emissions scenario, in which emissions from coal-fired electric generation units within the State of Michigan were reduced by 90 percent and all other mercury sources within the State of Michigan were reduced by 82 percent. The Calendar Year 2005 was modelled, as this was the year for which the MDEQ had developed an updated mercury emissions inventory for the state. Additionally, the project PIs also possessed daily event rainfall samples (i.e., mercury wet-deposition) for a number of sites (Detroit, Dexter, Flint, Grand Rapids, Pellston and Eagle Harbor, MI), as well as speciated ambient concentration data for two sites (Detroit and Dexter), all of which could therefore be used to evaluate the model performance. Unfortunately, due to problems with the wet-deposition sampling equipment at

the Flint, MI measurement site, gaps were present in the measured data and thus a comparison between measured and modeled wet-deposition was not included in this report. However, modeling results for the Flint site were included in the report to provide spatial representativeness of the presented results.

Hourly, three dimensional meteorological fields were modeled for Calendar Year 2005 using the Weather Research and Forecasting (WRF) model. The meteorological fields were then used in concert with the U.S. Environmental Protection Agency's (USEPA) 2005 National Emissions Inventory (and updated emissions provided for the State of Michigan by the MDEQ) as input into the Sparse Matrix Operator Kernel Emissions (SMOKE) Modeling System to generate hourly emissions of mercury and other important chemical species for the continental US, as well as parts of southern Canada and northern Mexico. Finally, these emissions (and the WRF model output) were used as input into the USEPA's Community Multi-scale Air Quality Model (CMAQ) to generate hourly ambient speciated mercury concentrations and deposition (both wet- and dry-) over the project's three modeling domains (36km, 12km and 4km). The latter domain (4km) focused upon the State of Michigan.

Overall, the largest total mercury deposition was predicated for the Detroit (Livernois) site, with 43.3 $\mu g/m^2$ (Wet: 17.7 $\mu g/m^2$, Dry: 25.6 $\mu g/m^2$), with Flint having the second highest total at 42.2 $\mu g/m^2$ (Wet: 13.4 $\mu g/m^2$, Dry: 28.8 $\mu g/m^2$). Total mercury deposition was predicted to decrease significantly for the locations that were more distant from local anthropogenic sources: Grand Rapids 19.9 $\mu g/m^2$ (Wet: 12.6 $\mu g/m^2$, Dry: 7.3 $\mu g/m^2$), Dexter 18.1 $\mu g/m^2$ (Wet: 10.1 $\mu g/m^2$, Dry: 8.0 $\mu g/m^2$), Eagle Harbor 16.2 $\mu g/m^2$ (Wet: 11.6 $\mu g/m^2$, Dry: 4.6 $\mu g/m^2$), and Pellston 13.5 $\mu g/m^2$ (Wet: 11.1 $\mu g/m^2$, Dry: 2.4 $\mu g/m^2$).

One additional component of the modeling effort was the tagging of specific emissions source categories, which were used to attribute the relative importance of the tagged source categories to the total mercury deposition within the State of Michigan. The results suggest that, in general, global sources of mercury represent the largest contributor to both wet- and dry-deposition for the selected locations within the State of Michigan that were highlighted in this report. Only at the two most urban sites that were highlighted (Detroit and Flint) did sources within the State of Michigan make a substantial contribution. In Detroit, sources from within the State of Michigan contributed 32 percent to the total mercury wet-deposition and 47 percent to the total mercury dry-deposition. In Flint, sources from within the State of Michigan contributed 19 percent to the total mercury wet-deposition and 54 percent to the total mercury dry-deposition. In Detroit, the largest contributions from tagged sources were waste incineration and coal-fired electric generation units. In Flint, waste incineration was by far the largest in-state contributor to the total mercury deposition there.

Finally, estimates were made as to the potential impact of a mercury emissions reduction strategy of reducing in-state coal-fired electric generating units by 90 percent and all other in-

state mercury emissions by 82 percent. Not surprisingly, the two sites that saw the most significant reduction in estimated total deposition were Detroit (Livernois) and Flint. The remaining sites, for which global sources were estimated to provide the dominant contribution, saw a limited reduction in total mercury deposition.

I. Meteorological Simulations

Methodology

The Weather Research and Forecasting (WRF) Model (http://www.wrf-model.org/index.php) was utilized to perform the simulation of hourly meteorological conditions for the Calendar Year 2005. The WRF Model is a next-generation mesoscale numerical weather prediction system that serves both operational forecasting and atmospheric research communities. This model is state-of-the-art, in that it is the core of one of the two primary weather forecasting models utilized by the U.S. National Centers for Environmental Prediction (NCEP). The WRF Model is suitable for applications across spatial scales ranging from meters to thousands of kilometers. The development of the WRF Model has been a collaborative partnership, principally among the National Center for Atmospheric Research (NCAR), the National Oceanic and Atmospheric Administration (NOAA), the National Centers for Environmental Prediction (NCEP) and the Forecast Systems Laboratory (FSL), the Air Force Weather Agency (AFWA), the Naval Research Laboratory, Oklahoma University, and the Federal Aviation Administration (FAA) (http://www.wrf-model.org/index.php). Unlike previous numerical weather prediction models which required supercomputing centers on which to run, WRF is now available for use by the broader research community and can be run on desktop workstations.

The WRF model was used to generate the hourly meteorological fields necessary to drive both the Sparse Matrix Operator Kernel Emissions (SMOKE) Modeling System (http://cmascenter.org/smoke/) and the Community Multi-scale Air Quality (CMAQ) model (http://www.cmascenter.org/cmaq/). The physical domains used for the simulations associated with this project were part of a nested grid configuration with a 36-km grid covering the continental United States and parts of Canada and Mexico, a 12-km grid covering the northeastern United States and a 4-km grid covering the Great Lakes watershed, including the State of Michigan (Figure 1). The use of a fine, 4-km grid over the Great Lakes allowed us to simulate the fine-scale influences of the five Great Lakes on the thermodynamic and wind flow patterns across the region. These influences can impact the dispersion, transport and fate of pollutants within the Great Lakes region, in general, and the State of Michigan, in particular.

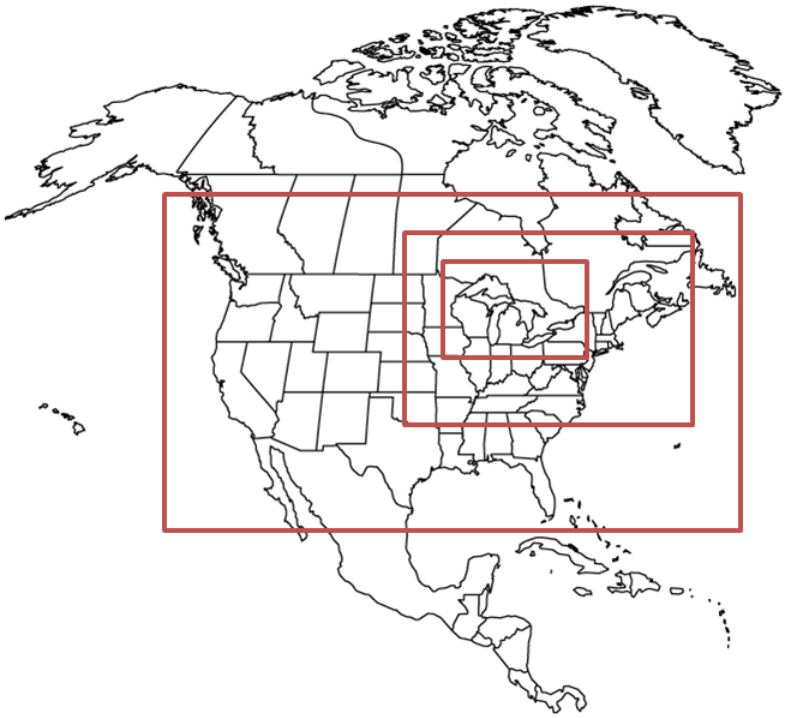

Figure 1. WRF modeling domain utilizing three nested domains: 36-km (CONUS), 12-km (northeastern US) and 04-km (Great Lakes watershed).

The WRF model was initialized using the North American Regional Reanalysis (NARR) dataset that is available for download from the National Climatic Data Center (http://nomads.ncdc.noaa.gov/). The WRF meteorological simulations were performed starting with the final week of 2004 in order to generate the meteorological fields necessary to perform a one-week "spin-up" of the CMAQ Regional Chemical Model. This CMAQ spin-up was performed to insure that the model was stable prior to the initiation of modeling for the first week of the period of interest, Calendar Year 2005. Subsequently, the WRF meteorological model was used to generate the hourly meteorological fields for the entire Calendar Year 2005. These simulations were performed in one-week steps, with each week's simulation having a 24-hour spin-up period using the last day of the previous week's simulation. The meteorological fields were archived for transfer to the Michigan Department of Environmental Quality (MDEQ), if desired.

Since some critical meteorological processes occur on size scales smaller than the model grid spacing (36, 12 and 4-km), these processes are accounted for in the WRF meteorological model through the use of a series of parameterization options. The options used for the Michigan TMDL simulations are provided in Table 1 below. These options were selected following a conversation with Dr. Greg Mann, Science Operations Officer for the National Weather Service Forecast Office in White Lake Michigan.

Table 1. WRF model parameterization options used for Michigan TMDL Study

Parameterization scheme	Scheme utilized in this project	Reference
Cloud microphysics	WSM 6-class graupel scheme	Hong and Lim (2006)
Longwave radiation	RRTM scheme	Mlawer *et al*. (1997)
Shortwave radiation	Dudhia scheme	Dudhia (1989)
Atmospheric boundary layer	Yonsei University scheme	Hong *et al*. (2006)
Atmospheric surface layer	Monin-Obukhov scheme	Monin and Obukhov (1954)
Land surface processes	Unified Noah land surface scheme	Tewari *et al*. (2004)
Cumulus physics**	Kain-Fritsch scheme	Kain (2004)

** A cumulus physics parameterization scheme is not typically used at model resolutions of 4km or less. Instead, the model is allowed to explicitly describe cumulus processes by itself.

Pre-simulation Sensitivity Evaluations

Sensitivity to use of a cumulus parameterization scheme in 4km domain

One typically does not include a parameterization of cumulus physics for grid sizes 4km or less, as the model is allowed to explicitly describe cumulus processes by itself. As a short verification exercise, we performed two WRF simulations for the period of 13-16 September 2005 for our 4km domain. One simulation included the use of a cumulus parameterization for the 4km domain (Kain-Fritsch scheme) and the second simulation did not include the use of a cumulus parameterization scheme. Using the final 48-hours of the 96-hour period as a test data set for comparison between the "with cumulus physics parameterization" and "without cumulus physics parameterization" simulations, we compared the output for the 0000 UTC and 1200 UTC hours for each of the two days (15 and 16 September 2005). No difference was found in the domain-wide mean values (N=14 sites for comparison) of the following variables that were evaluated using the Meteorological Evaluation Tool Version 3.0 (METv3.0) POINT STAT analysis:

a. 500-mb height
b. 500-mb temperature
c. 500-mb specific humidity
d. 850-mb height
e. 850-mb temperature
f. 850-mb specific humidity

Additionally, we performed an analysis using the METv3.0 MODE analysis tool which computed the distances between the centroids of the precipitation areas generated by the WRF model simulations "with cumulus physics parameterization" and "without cumulus physics parameterization" and the observed precipitation areas. Again, the time period analyzed was 15 and 16 September 2005, with the results summarized below:

Table 2. Results of METv3.0 MODE Precipitation Analysis for Cumulus Parameterization Sensitivity Analysis

	With Cumulus Parameterization	Without Cumulus Parameterization
Average Centroid Distance (km):	116	99
Standard Deviation (km):	78	67
Median (km):	90	79
Number of precipitation areas:	32	29

The mode analysis suggested that the average difference in distance between the centroids of the observed and model precipitation areas were less for the cases in which a cumulus parameterization scheme was not used.

Combined, the results obtained for the METv3.0 POINT STAT and MODE analyses did not provide evidence that our domain average results would be adversely impacted by following the traditional approach of not utilizing a cumulus physics parameterization scheme for our 4km domain. Therefore, we did not utilize the cumulus physics parameterization scheme for our 4km domain.

<u>Sensitivity to use of different cloud microphysics and land surface parameterization schemes</u>

A series of short-term (96-hour) WRF meteorological simulations were performed using different combinations of model parameterization options in order to test the sensitivity of the model to the parameterization options used in the BASE CASE simulations (Table 1). The combinations used in these sensitivity evaluations are listed in Table 3, with the BASE CASE set of parameterization schemes designated as P4 in Table 3. The parameterization schemes utilized are primarily those used in the BASE CASE simulations. The two parameterization categories in the sensitivity analyses were the cloud microphysics and land surface categories. The additional parameterization schemes used during the evaluation were cloud microphysics scheme "WRF Single-moment 3-Class Scheme" (Hong *et al*., 2004) and the land surface scheme "Five-layer Thermal Diffusion Scheme" (Dudhia, 1996). The evaluation was run for three, four-day periods (which included one 24 hour spin-up day):

(a) January 09-12, 2005
(b) June 06-09, 2005
(c) September 13-16, 2005

Simulations were performed for all days and all four parameterization sets using the NARR data set as input. The results presented in Table 4 represent an evaluation from our 36km domain simulations for the final day of each four day period indicated above.

Table 3. WRF model parameterization options using NARR model initial and boundary conditions.

Parameterization scheme	P1	P2	P3	P4
Cloud microphysics	WSM 3-class	WSM 3-class	WSM 6-class	WSM 6-class
Longwave radiation	RRTM	RRTM	RRTM	RRTM
Shortwave radiation	Dudhia	Dudhia	Dudhia	Dudhia
Atmospheric boundary layer	Yonsei University	Yonsei University	Yonsei University	Yonsei University
Atmospheric surface layer	Monin-Obukhov	Monin-Obukhov	Monin-Obukhov	Monin-Obukhov
Land surface processes	Thermal Diffusion	Unified Noah	Thermal Diffusion	Unified Noah
Cumulus physics**	Kain-Fritsch	Kain-Fritsch	Kain-Fritsch	Kain-Fritsch

** A cumulus physics parameterization scheme is not typically used at model resolutions of 4km or less. Instead, the model is allowed to explicitly describe cumulus processes by itself.

Table 4. WRF model parameterization evaluation results

(a) Comparison of results for 12 January 2005

DAY 4 NARR P1									
0000 UTC	0000 UTC	0000 UTC	0000 UTC	0000 UTC	0000 UTC	1200 UTC	1200 UTC	1200 UTC	1200 UTC
Height	Variable	Matches	Fcst Mean	Obs Mean	Mean Err	Matches	Fcst Mean	Obs Mean	Mean Err
P500	HGT	82	5554	5553	1	87	5573	5566	7
P500	TMP	82	251	252	-1	87	253	253	-1
P500	SPFH	82	0.001	0.001	0.000	87	0.001	0.001	0.000
P850	HGT	82	1446	1430	16	87	1452	1432	19
P850	TMP	76	275	275	0	78	275	276	-1
P850	SPFH	76	0.004	0.004	0.000	78	0.004	0.004	0.000
P1000	SPFH	29	0.007	0.006	0.000	32	0.007	0.007	0.000

DAY 4 NARR P2									
0000 UTC	0000 UTC	0000 UTC	0000 UTC	0000 UTC	0000 UTC	1200 UTC	1200 UTC	1200 UTC	1200 UTC
Height	Variable	Matches	Fcst Mean	Obs Mean	Mean Err	Matches	Fcst Mean	Obs Mean	Mean Err
P500	HGT	82	5555	5553	2	87	5575	5566	8
P500	TMP	82	251	252	-1	87	253	253	-1
P500	SPFH	82	0.001	0.001	0.000	87	0.001	0.001	0.000
P850	HGT	82	1448	1430	18	87	1453	1432	21
P850	TMP	76	275	275	0	78	275	276	-1
P850	SPFH	76	0.004	0.004	0.000	78	0.004	0.004	0.000
P1000	SPFH	29	0.007	0.006	0.000	32	0.007	0.007	0.000

DAY 4 NARR P3									
0000 UTC	0000 UTC	0000 UTC	0000 UTC	0000 UTC	0000 UTC	1200 UTC	1200 UTC	1200 UTC	1200 UTC
Height	Variable	Matches	Fcst Mean	Obs Mean	Mean Err	Matches	Fcst Mean	Obs Mean	Mean Err
P500	HGT	82	5556	5553	3	87	5573	5566	7
P500	TMP	82	252	252	-1	87	253	253	0
P500	SPFH	82	0.001	0.001	0.000	87	0.001	0.001	0.000
P850	HGT	82	1440	1430	10	87	1445	1432	13
P850	TMP	76	275	275	0	78	275	276	-1
P850	SPFH	76	0.004	0.004	0.000	78	0.004	0.004	0.001
P1000	SPFH	29	0.007	0.006	0.001	32	0.007	0.007	0.000

DAY 4 NARR P4									
0000 UTC	0000 UTC	0000 UTC	0000 UTC	0000 UTC	0000 UTC	1200 UTC	1200 UTC	1200 UTC	1200 UTC
Height	Variable	Matches	Fcst Mean	Obs Mean	Mean Err	Matches	Fcst Mean	Obs Mean	Mean Err
P500	HGT	82	5557	5553	4	87	5575	5566	8
P500	TMP	82	252	252	-1	87	253	253	0
P500	SPFH	82	0.001	0.001	0.000	87	0.001	0.001	0.000
P850	HGT	82	1442	1430	12	87	1447	1432	14
P850	TMP	76	275	275	0	78	275	276	-1
P850	SPFH	76	0.004	0.004	0.000	78	0.004	0.004	0.001
P1000	SPFH	29	0.007	0.006	0.000	32	0.007	0.007	0.000

(b) Comparison of results for 09 June 2005

DAY 4 NARR P2									
0000 UTC	0000 UTC	0000 UTC	0000 UTC	0000 UTC	0000 UTC	1200 UTC	1200 UTC	1200 UTC	1200 UTC
Height	Variable	Matches	Fcst Mean	Obs Mean	Mean Err	Matches	Fcst Mean	Obs Mean	Mean Err
P500	HGT	80	5757	5754	3	83	5773	5763	10
P500	TMP	80	261	261	-1	83	261	261	0
P500	SPFH	80	0.001	0.001	0.000	83	0.001	0.001	0.000
P850	HGT	81	1483	1478	5	83	1502	1490	12
P850	TMP	74	288	288	-1	76	287	287	-1
P850	SPFH	74	0.008	0.008	0.000	76	0.008	0.008	0.000
P1000	SPFH	26	0.012	0.012	0.000	28	0.012	0.013	-0.001

DAY 4 NARR P3									
0000 UTC	0000 UTC	0000 UTC	0000 UTC	0000 UTC	0000 UTC	1200 UTC	1200 UTC	1200 UTC	1200 UTC
Height	Variable	Matches	Fcst Mean	Obs Mean	Mean Err	Matches	Fcst Mean	Obs Mean	Mean Err
P500	HGT	80	5758	5754	4	83	5774	5763	11
P500	TMP	80	261	261	0	83	261	261	0
P500	SPFH	80	0.001	0.001	0.000	83	0.001	0.001	0.000
P850	HGT	81	1478	1478	0	83	1497	1490	7
P850	TMP	74	288	288	0	76	287	287	0
P850	SPFH	74	0.008	0.008	0.000	76	0.008	0.008	0.000
P1000	SPFH	26	0.011	0.012	0.000	28	0.012	0.013	-0.001

DAY 4 NARR P4									
0000 UTC	0000 UTC	0000 UTC	0000 UTC	0000 UTC	0000 UTC	1200 UTC	1200 UTC	1200 UTC	1200 UTC
Height	Variable	Matches	Fcst Mean	Obs Mean	Mean Err	Matches	Fcst Mean	Obs Mean	Mean Err
P500	HGT	80	5756	5754	2	83	5771	5763	8
P500	TMP	80	261	261	0	83	261	261	0
P500	SPFH	80	0.001	0.001	0.000	83	0.001	0.001	0.000
P850	HGT	81	1476	1478	-1	83	1496	1490	6
P850	TMP	74	288	288	0	76	287	287	0
P850	SPFH	74	0.008	0.008	0.000	76	0.008	0.008	0.000
P1000	SPFH	26	0.012	0.012	0.000	28	0.012	0.013	-0.001

Data for DAY 4 NARR P1 was not available.

(c) Comparison of results for 16 September 2005

DAY 4 NARR P1									
0000 UTC	0000 UTC	0000 UTC	0000 UTC	0000 UTC	0000 UTC	1200 UTC	1200 UTC	1200 UTC	1200 UTC
Height	Variable	Matches	Fcst Mean	Obs Mean	Mean Err	Matches	Fcst Mean	Obs Mean	Mean Err
P500	HGT	84	5806	5814	-8	87	5814	5818	-4
P500	TMP	84	262	263	-1	87	262	263	-1
P500	SPFH	84	0.001	0.001	0.000	86	0.001	0.001	0.000
P850	HGT	84	1524	1527	-3	88	1538	1529	9
P850	TMP	78	288	288	0	82	287	288	-1
P850	SPFH	78	0.008	0.008	0.000	81	0.008	0.008	0.000
P1000	SPFH	29	0.014	0.013	0.000	32	0.013	0.013	0.000

DAY 4 NARR P2									
0000 UTC	0000 UTC	0000 UTC	0000 UTC	0000 UTC	0000 UTC	1200 UTC	1200 UTC	1200 UTC	1200 UTC
Height	Variable	Matches	Fcst Mean	Obs Mean	Mean Err	Matches	Fcst Mean	Obs Mean	Mean Err
P500	HGT	84	5805	5814	-9	87	5814	5818	-4
P500	TMP	84	262	263	-1	87	262	263	-1
P500	SPFH	84	0.001	0.001	0.000	86	0.001	0.001	0.000
P850	HGT	84	1525	1527	-2	88	1539	1529	11
P850	TMP	78	288	288	0	82	287	288	-1
P850	SPFH	78	0.008	0.008	0.000	81	0.008	0.008	0.000
P1000	SPFH	29	0.014	0.014	0.000	32	0.013	0.013	0.000

DAY 4 NARR P3									
0000 UTC	0000 UTC	0000 UTC	0000 UTC	0000 UTC	0000 UTC	1200 UTC	1200 UTC	1200 UTC	1200 UTC
Height	Variable	Matches	Fcst Mean	Obs Mean	Mean Err	Matches	Fcst Mean	Obs Mean	Mean Err
P500	HGT	84	5805	5814	-9	87	5814	5818	-4
P500	TMP	84	262	263	-1	87	262	263	-1
P500	SPFH	84	0.001	0.001	0.000	86	0.001	0.001	0.000
P850	HGT	84	1520	1527	-6	88	1535	1529	6
P850	TMP	78	288	288	0	82	287	288	-1
P850	SPFH	78	0.008	0.008	0.000	81	0.008	0.008	0.000
P1000	SPFH	29	0.014	0.014	0.001	32	0.013	0.013	0.000

DAY 4 NARR P4									
0000 UTC	0000 UTC	0000 UTC	0000 UTC	0000 UTC	0000 UTC	1200 UTC	1200 UTC	1200 UTC	1200 UTC
Height	Variable	Matches	Fcst Mean	Obs Mean	Mean Err	Matches	Fcst Mean	Obs Mean	Mean Err
P500	HGT	84	5805	5814	-9	87	5815	5818	-3
P500	TMP	84	262	263	-1	87	262	263	-1
P500	SPFH	84	0.001	0.001	0.000	86	0.001	0.001	0.000
P850	HGT	84	1522	1527	-5	88	1536	1529	7
P850	TMP	78	288	288	0	82	287	288	0
P850	SPFH	78	0.008	0.008	0.000	81	0.008	0.008	0.000
P1000	SPFH	29	0.014	0.014	0.001	32	0.014	0.013	0.001

From the above analysis, there was no evidence that there was a marked improvement in the domain wide performance as a result of using specific cloud microphysics or land use schemes different than those used in the BASE CASE (P4). As a result, our initial BASE CASE parameterization set was maintained for use in our simulations.

WRF-Simulation Evaluations

Following the performance of the WRF meteorological simulations, we performed a series of analyses to evaluate the WRF model's performance. In the original project plan, our goal was to evaluate the performance of the WRF model for Calendar Year 2005, with the plan to consider re-running the simulations should results not meet certain evaluation criteria. For these evaluations, we proposed to perform both qualitative and quantitative evaluations.

The stated goal of these evaluations of model performance was to determine if there was a systematic bias in the model that exceeded our acceptance criteria, and then to consider

initializing the model with a different input meteorological data set, such as the North American Mesoscale (NAM) model, as one option for attempting to improve the model performance obtained using the NARR as the input meteorological data set. Due to delays in the start of the project and the project deadline for the State of Michigan needing our model results, the project Principal Investigator (PI) and the UM project Quality Assurance (QA) Manager determined that there would not be time to run the WRF meteorological model a second time. As a result, the evaluations that were performed would be used to understand the performance of the model and the uncertainties that were likely introduced into the CMAQ regional chemical modeling results due to these uncertainties.

Qualitative Evaluations

For the qualitative comparisons between the WRF model output and observed meteorological fields, we chose to compare the modeled versus observed conditions at both the surface and 500 millibar levels at 1200 Universal Coordinated Time (UTC) for each day modeled. The purpose of the qualitative comparisons was to evaluate the model's overall ability to simulate the large scale (on the order of 1000 km) weather patterns which influence atmospheric transport and precipitation processes. At the surface level, qualitative evaluations that were to be performed included the presence/magnitude of centers of high/low pressure, location of cold/warm frontal boundaries and general areal extent of precipitation boundaries. At the 500 millibar level, qualitative evaluations set to be performed included the general location and magnitude of geopotential height field ridges and troughs.

Table 5. Evaluation criteria and levels of acceptance for WRF model output results.

Model Level	Model Field Evaluated	Evaluation Acceptance Criteria
Surface	Surface Pressure Centers	Within 100km of observed location
Surface	Frontal Boundary Positions	Within 100km of observed location
Surface	Areal coverage of precipitation	Centroid within 100km of observed locations
500 millibar	Trough/Ridge Axes Location	Axes within 250km of observed locations
500 millibar	Trough/Ridge Magnitude	Maxima/minima within 120m

Given that the 4km domain seemed too small to provide an ample sample size, we chose to focus our evaluation efforts on the 12km domain. When performing the qualitative evaluations, we ran into a number of issues with the evaluations for frontal boundary positions, 500 millibar trough/ridge axes locations and trough/ridge magnitudes. Namely, for a given surface frontal boundary, the difference between observation and model prediction would often vary considerably along the length of the frontal boundary. For the 500 millibar trough/ridge features, we often observed significant periods during which troughs/ridges did not exist even within our 12km domain, making these evaluations difficult, as well. However, we did feel that we were

able to observe a significant number of surface low pressure systems and precipitation events across our 12km domain such that these measures could be obtained.

Sea Level Pressure Spatial Analysis

Using the Integrated Data Viewer (IDV) application (http://www.unidata.ucar.edu/software/idv/docs/userguide/), maps were created to verify model performance on the placement of low pressure centers at mean sea level at 1200 UTC for each day. The maps were then imported into Google Earth, where the centroid distance between the observed low and the model low were calculated. The yearly aggregated results shown in Table 6 are the average distance measured between the centroid in kilometers, the percentage of days in which the centroid distance met the criteria of being less than 100 km, and the average and median differences between the lowest observed and lowest forecasted pressure.

Table 6. MSLP Spatial Analysis. Distances measured in kilometers, pressure measured in millibars.

Differences in Low Pressure Center at MSLP	
Average centroid distance	326 kilometers
Percentage of days meeting criteria	12.1%
Average lowest pressure difference	-0.1 mb
Median lowest pressure difference	0.0 mb

These results suggest that the model did a good job of predicting the magnitude of the low pressure center, however the location of the center was often not predicted accurately. In many cases, the differences in the positions of the observed/modeled centers of low pressure were the result of the fact that the areas of low pressure were spatially broad in nature. Therefore, there were times in which the general placement of the low pressure areas was correct, but the exact locations of the lowest pressure were not correct.

MODE Results

The METv3 MODE analysis tool was used to verify model performance on the accuracy of the model forecast location of areas of precipitation. The output from the tool was exported, and the distance between the centroids of forecast and observed objects (that is, areas of precipitation) were calculated using the Haversine great circle formula and aggregated on a monthly basis. Table 7 shows the average distance between forecast and observed precipitation clusters, the number of clusters compared for each month, and the percentage of clusters for which the centroid distance was less than the 100 km criteria.

Table 7. Results of METv3.0 MODE Precipitation Analysis for 2005 WRF BASE CASE Simulations

	Jan	Feb	Mar	Apr	May	Jun	Jul	Aug	Sep	Oct	Nov	Dec
Avg. Centroid Distance (km)	112	118	103	117	92	93	81	92	104	101	117	116
Object Count	48	39	72	112	160	235	280	221	108	93	59	54
Percentage Meet Criteria	43.75	46.2	56.9	43.75	62.5	61.3	66.8	61.1	56.5	58.0	49.2	42.6

As can be seen, there was a distinct seasonality to the performance of the model with respect to the precipitation forecasts. During the "warm season" (May through September), over 60 percent of the observed precipitation clusters met the average centroid distance threshold criteria, while less than 60 percent of the observed precipitation clusters met the average centroid distance threshold criteria during the "cold season" (September through April). One potential explanation for this observation is that during the colder part of the year, the majority of precipitation events are of the spatially broader stratiform variety. The spatially broad nature of the precipitation would allow for a greater error in forecasted centroid location. During the "warm season", when convective precipitation plays a greater role, a smaller spatial area is typically conducive to convection and thus the modeled and observed precipitation clusters might be expected to be closer in centroid location. That said, even during the "cold season", the average centroid difference was very close to the 100 km threshold, giving confidence that the model did a reasonable job of predicting the location of observed precipitation.

While the WRF model did a reasonable job of modeling the observed precipitation location, the model had a significant "wet bias" for our key sampling locations (Figure 2). For these locations, there was an average over-prediction of annual precipitation of 63 percent, with the model predicting twice as much precipitation than observed at the Eagle Harbor site. It is difficult to pinpoint the exact reason for the wet bias in the model for this period. For example, the WRF model's wet bias in our simulations could be associated with large errors associated with a few large precipitation events. Additionally, the wet bias could be due to systematic biases in model soil moisture, the latter of which could influence both the modeled temperature and moisture in the planetary boundary layer. The result of these latter biases would be the potential for over-estimation of precipitation, and thus of wet-deposition of total mercury, to the sites.

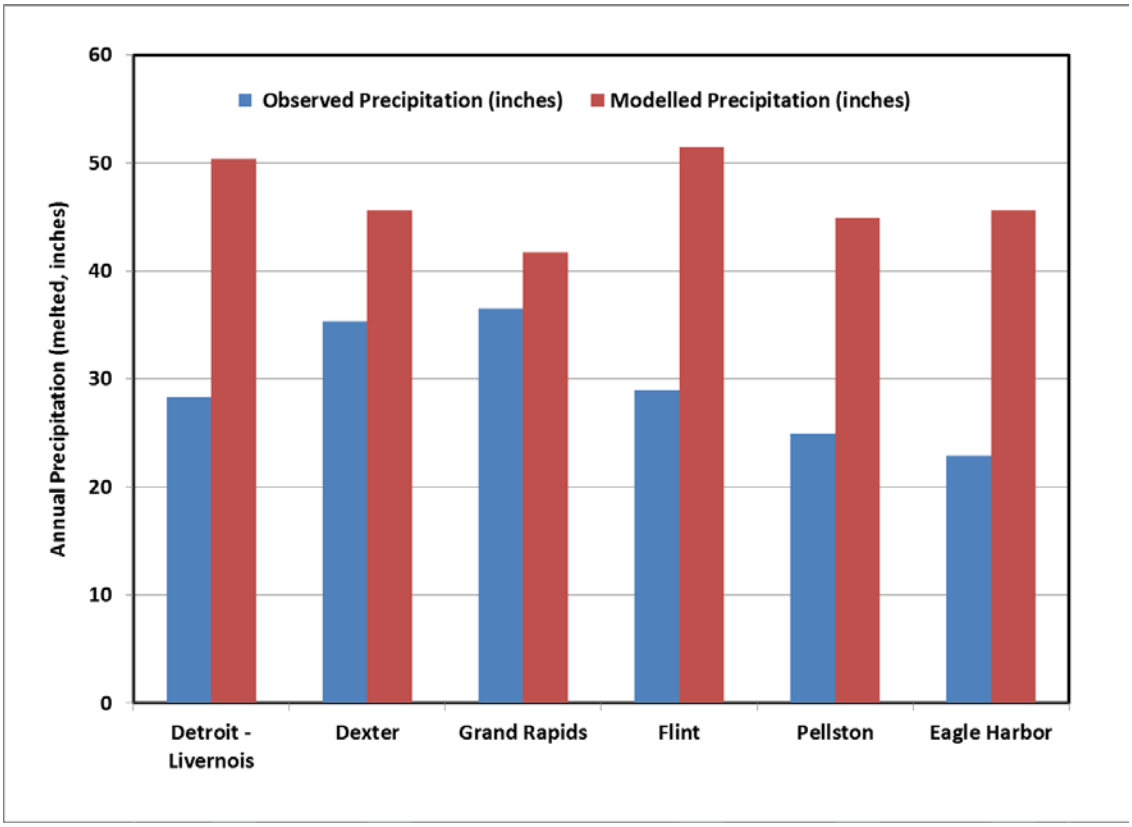

Figure 2. Comparison of modeled and measured precipitation for select locations within 4km modeling grid for Calendar Year 2005 WRF BASE CASE simulation**.**

Quantitative Evaluations

For the quantitative comparisons between the WRF model output and the observed meteorological fields, we again used the METv3 software package that was developed by the Developmental Testbed Center (DTC) at the National Center for Atmospheric Research in Boulder, Colorado. According to the DTC, METv3 provides the numerical prediction community with common software incorporating the latest advances in atmospheric model verification.

METv3 provides a variety of verification techniques, including:

- Standard verification scores comparing gridded model data to point-based observations
- Standard verification scores comparing gridded model data to gridded observations
- Spatial verification methods comparing gridded model data to gridded observations using neighborhood, object-based, and intensity-scale decomposition approaches

For this project, we proposed to use a number of measures to evaluate the model performance. These measures were consistent with those suggested in USEPA QA/G-9R (2006a) and USEPA QA/G-9S (2006b) and included:

1. Scatter plots (model vs. observation) of twelve-hourly (00 and 12 UTC) surface and 850-mb temperature, specific humidity and wind speed by month.

a. This information would provide a general measure of any potential biases in the prediction of these fields.

b. Slope, intercept and Pierson correlation coefficients would be determined for each plot.

c. *Evaluation criteria*: Pierson correlation coefficients of less than r=0.5 would represent a sufficient deviation in model performance from observation to require a further review of data to determine the cause of this deviation.

2. Monthly average, standard deviation, 10th- and 90th-percentiles and mean absolute error would be computed using twelve-hourly (00 and 12 UTC) surface and 850-mb temperature, specific humidity and wind speed by month.

   a. This information would provide us with an evaluation as to how well the model handled the average and range of conditions observed each month throughout the year.

   b. *Evaluation criteria*: While the monthly average, standard deviation, 10th- and 90th-percentiles would provide us with a general statistical measure of the performance of our model versus observations, the mean absolute error (MAE) would be used determine if the model performance was varying from observations at a significant level such that consideration of corrective actions might be necessary. If the following threshold criteria were exceeded, the UM Project Manager will then contact the USEPA Technical Contact to discuss what, if any, actions should be pursued.

      i. Temperature criteria: Corrective action required if MAE exceeds 3.0ºK.

      ii. Specific humidity criteria: Corrective action required if MAE exceeds 3.0 grams/kilogram.

      iii. Wind speed criteria: Corrective action required if MAE exceeds 5 m/sec.

Given that the project start date was delayed, the WRF Model results were not able to be evaluated until the project was fully underway. As a result, any observed errors or biases outside the expressed thresholds were not utilized to drive any corrective actions associated with the modeling activities, but rather were used to describe the levels of uncertainty associated with those variables and their potential impact on the overall results.

Point Stat Results

The METv3 POINT STAT tool was used to evaluate the WRF model's performance at predicting the temperature, specific humidity, and wind speed at two atmospheric levels – surface, and 850 mb. These two levels were chosen given they provide important measures within the planetary boundary layer. Often ranging in depth between hundreds of meters to 3000 meters, the planetary boundary layer is that layer into which pollutants are emitted and locally transported, transformed and deposited.

One measure of a model's ability to accurately reproduce observed atmospheric conditions is the model's ability to accurately explain the temporal and spatial variability in those conditions. As

a result, for our Calendar Year 2005 simulations, each observation was paired to a forecast from the model, and results were aggregated on a monthly basis, with a linear trend line and the Pierson correlation coefficient was calculated for each variable for each month. The correlation coefficients are shown in Table 8, with cells highlighted in yellow representing variables for which the criteria of the correlation coefficient being greater than 0.5 was not met. Overall, the correlation results were satisfactory, with only three monthly periods having correlation coefficients that did not meet the 0.5 acceptance criteria (surface wind speed for June and August 2005 and 850-mb wind speed for August 2005). In general, the correlations for the wind speed (both surface and 850-mb) were lower than those for the specific humidity and temperature. For these latter two variables, the model was able to explain well over 50 percent of the observed variability. It is not too surprising that the correlations for the specific humidity and temperature at both levels were greater than those obtained for the wind speed, as specific humidity and temperature typically are less spatially variable and thus fine scale variations are less prominent and thus less likely to contribute to lower correlations.

Table 8. Values given are Pierson Correlation coefficients, with highlighted cells indicating r>0.5 evaluation criteria not met.

	Surface Specific Humidity	Surface Temperature	Surface Wind Speed	850-mb Specific Humidity	850-mb Temperature	850-mb Wind Speed
Jan	0.93	0.91	0.72	0.87	0.96	0.76
Feb	0.88	0.87	0.62	0.62	0.94	0.65
Mar	0.91	0.89	0.51	0.81	0.95	0.69
Apr	0.89	0.85	0.62	0.77	0.92	0.65
May	0.86	0.85	0.62	0.68	0.93	0.57
Jun	0.82	0.75	0.46	0.56	0.86	0.52
Jul	0.81	0.78	0.54	0.63	0.89	0.52
Aug	0.79	0.77	0.30	0.56	0.87	0.40
Sep	0.74	0.75	0.55	0.56	0.88	0.55
Oct	0.91	0.85	0.63	0.77	0.93	0.62
Nov	0.88	0.87	0.60	0.75	0.92	0.62
Dec	0.86	0.83	0.57	0.74	0.93	0.62

Another measure of a model's ability to describe observed atmospheric conditions is the ability of the model not only to accurately describe the atmospheric phenomenon's variability, but also to accurately describe its magnitude. For example, in the case of regional chemical transport modeling, accurate representation of wind flow (using wind speed as a surrogate) is important given its role in the transport of pollutants and their precursors. Temperature impacts stability and precipitation type, while specific humidity impacts cloud formation (and thus radiative transfer through the atmosphere) and subsequently precipitation formation and amounts. As a result, for our Calendar Year 2005 simulations, each observation was paired to a forecast from the model and the monthly mean absolute error was calculated for 00 UTC and 12 UTC. The results are presented in Table 9 below, with monthly mean absolute errors not meeting the threshold criteria being highlighted in yellow. In this case, the surface and 850-mb specific

humidity and wind speeds fell within the accept error thresholds. However, the monthly mean absolute errors often fell outside the acceptable threshold for the surface temperature forecasts.

Following this analysis, we chose to look further into the errors associated with the surface and 850-mb temperatures. Following calculation of the mean error (as opposed to mean absolute error), it would found that the modeled surface temperature was predominantly cooler than the observed temperatures, regardless of season or time of day. It is interesting to note that while the annual mean error at 12 UTC (morning) was relatively small (-0.3 deg K), the annual mean error at 00 UTC (early evening) was relatively large (-2.0 deg K). The annual mean error in the 850-mb temperature forecasts also suggested that the modeled temperature was cooler than the observed temperatures at this level. In contrast, however, the annual mean error at 850-mb was consistent between the 00 UTC and 12 UTC times (-0.6 deg K for both times). Given that the layer between the surface and 850-mb (nominally, 1500 meters deep) is considered to be representative of the planetary boundary layer described above, the aforementioned temperature biases may have had an impact on the stability of this layer. Namely, if the modeled surface temperatures were considerably cooler than those observed, this could have resulted in a more stable planetary boundary layer and thus less mixing in the model than was actually observed. This, in turn, could have resulted in modeled concentrations that were greater than those observed for locations near local sources.

Table 9. Mean Absolute Error for 00Z and 12Z Model/Observation Comparisons for the 12km Domain

Mean Absolute Error	January		February		March		April		May		June	
	00 UTC	12 UTC	00 UTC	12 UTC	00 UTC	12 UTC	00 UTC	12 UTC	00 UTC	12 UTC	00 UTC	12 UTC
Surface Temperature (Deg K)	3.4	3.6	4.1	3.3	4.4	2.9	3.7	2.2	3.4	2.1	3.3	2.4
Surface Specific Humidity (g/kg)	0.6	0.6	0.7	0.6	0.6	0.5	0.9	0.8	1.0	0.9	1.6	1.5
Surface Wind Speed (m/sec)	2.7	2.5	2.9	2.7	3.6	3.1	2.9	3.3	2.6	2.3	2.6	2.4
850mb Temperature (Deg K)	2.1	2.3	2.1	2.2	2.1	2.1	2.3	2.2	1.9	1.9	1.8	1.8
850mb Specific Humidity (g/kg)	0.8	0.8	0.9	1.0	0.7	0.8	1.0	1.1	1.1	1.3	1.9	2.0
850mb Wind Speed (m/sec)	3.1	3.1	3.4	3.4	3.2	3.4	3.1	3.5	3.0	3.3	3.1	3.3

Mean Absolute Error	July		August		September		October		November		December	
	00 UTC	12 UTC	00 UTC	12 UTC	00 UTC	12 UTC	00 UTC	12 UTC	00 UTC	12 UTC	00 UTC	12 UTC
Surface Temperature (Deg K)	3.2	2.1	3.4	2.4	3.7	3.0	2.8	2.7	2.9	2.8	3.0	3.1
Surface Specific Humidity (g/kg)	1.9	1.9	1.9	1.9	1.7	2.0	1.1	1.1	1.0	1.0	0.6	0.7
Surface Wind Speed (m/sec)	2.4	2.1	2.9	2.9	3.0	2.9	3.0	2.8	3.0	2.9	2.9	2.6
850mb Temperature (Deg K)	1.5	1.6	1.8	1.8	1.8	1.8	1.7	1.9	2.1	2.3	2.2	2.3
850mb Specific Humidity (g/kg)	1.9	2.0	1.9	2.2	2.2	2.3	1.4	1.5	1.1	1.1	0.6	0.7
850mb Wind Speed (m/sec)	2.7	3.0	3.1	3.5	3.5	3.6	3.1	3.4	3.3	3.8	3.4	3.5

One potential reason that the modeled surface temperatures may have been cooler than those observed is the fact that the model produced greater precipitation than was observed, thus potentially resulting in a moister soil than observed. If this occurred, the added moisture in the soil would have reduced the amount of incident solar radiation that was available to heat the atmosphere, given that a large percentage of that radiation would have been partitioned into evaporating the excess moisture at the surface.

II. Emissions Processing

Methodology – Raw Emissions Input Files

For the CMAQ Regional Chemical Model effort, we utilized the 2005 USEPA National Emissions Inventory Version 4.1 (hereafter, 2005 NEIv4.1) for both Criteria Air Pollutants and Hazardous Air Pollutants (USEPA, 2005). The inventory can be obtained publicly, at no cost, by accessing the following website:

http://www.epa.gov/ttn/chief/emch/index.html

The 2005 NEIv4.1, which includes the emissions of mercury [either as total mercury, gaseous elemental mercury (GEM), gaseous oxidized mercury (GOM) and particle bound mercury (PBM)], is broken into area, nonroad mobile, onroad mobile and point source sectors. The mercury emissions for the State of Michigan within the inventory were updated with new emissions estimates which had been developed after the release of the 2005 NEIv4.1. The data used to update the inventory was obtained from the:

- Michigan Department of Environmental Quality's "2005 Estimates of Anthropogenic Mercury Air Emissions in Michigan" (MDEQ, 2011), and
- Michigan Department of Environmental Quality's Michigan Air Emissions Reporting System (MAERS) data.

The anthropogenic area source emissions reported within the "2005 Estimates of Anthropogenic Mercury Air Emissions in Michigan" (MDEQ, 2011) were developed using a "flow pathway" approach that was developed by the Swedish Nation Chemicals Inspectorate (KEMI), which estimated releases from batteries, fluorescent lamps and sewage sludge. The flow pathway was further refined for Wisconsin and Minnesota by Barr Engineering Company (Wisconsin Department of Natural Resources, 2006).

These revised total mercury emissions estimates for anthropogenic area sources within the State of Michigan were provided to us by the MDEQ as a statewide total, with an assumed speciation as gaseous elemental mercury (GEM). Anthropogenic area source emissions are generally reported on a "per county" basis in the 2005 NEIv4.1. In order to update the 2005 NEIv4.1 anthropogenic area source emissions for mercury for the State of Michigan, the MDEQ's updated estimated statewide total (1308 lbs/yr) was distributed across the state by using county population estimates based upon the U.S. Census Bureau, Estimated Population of Counties for April 2000 to July 2005 (U.S. Census Bureau, 2005). As an example, according to the U.S. Census Bureau (2005), Genessee County, MI contained 4.4 percent of the state's population. Therefore the total anthropogenic area source emissions from Genessee County were estimated to be 4.4 percent of the 1308 lbs/yr statewide total, or 57.4 lbs/yr. Within the raw emissions files themselves, the emissions were reported in tons/yr, which is the standard unit of emissions reported in the 2005 NEIv4.1. These updated emissions are included in the following file:

arinv_nonpt_pf4_hap_nopfc_nobafmpesticidesplus_28may2010_v1_rev083012_orl.txt

Point source emissions within the State of Michigan were also updated based upon data provided to the project team by the MDEQ and originating from the State of Michigan's MAERS database. The files which were updated include:

ptinv_2005_ICR_BoilerMACT_Hg_ptnonipm_20aug2010_v0_rev080212_orl.txt
ptinv_2005_ptnonipm_natahg_minus_boilermacticr_17aug2010_v0_rev082412_orl.txt
ptinv_2005_ptipm_natahg_minus_boilermacticr_17aug2010_v0_rev073112_orl.txt

These files represented updated estimates of mercury emissions for the 2005 NEIv4.1, which replace mercury emissions previously included in the following files:

ptinv_ptipm_hap2005v2_allHAPs_revised12mar2009_14jul2010_v1_rev080812_nohg_orl.txt
ptinv_ptnonipm_hap2005v2_revised_08jul2010_v2_rev080812_nohg_orl.txt

Unfortunately, in the distribution of the 2005 NEIv4.1, the USEPA kept the original emissions estimates of mercury in these files. Thus, to avoid double counting mercury emissions, the emission of mercury were removed from these files.

Biogenic emissions of mercury were not provided as part of the 2005 NEIv4.1. However, based upon the work of Wiedinmyer and Friedli (2007), the project team developed estimates of GEM emissions from wildfires based upon the suggesting scaling of gaseous elemental mercury emissions with CO emissions from wildfires. This scaling was applied to CO emissions estimates from wildfires that were provided as part of the 2005 USEPA NEIv4.1 emissions inventory. The biogenic emissions of mercury from wildfires was include in the following file:

arinv_avefire_2002ce_21dec2007_v1_withhg_ida.txt

Emissions databases for both Canadian and Mexican sources were also available from the USEPA Emissions Modeling Clearinghouse website (www.epa.gov/ttn/chief/emch/index.html). However, the 2005 USEPA NEIv4.1 distribution did not include a mercury emissions inventory for Mexico. As a result, the project team developed an emissions inventory file for Mexico by taking reported national emissions for Mexico (Acosta-Ruiz and Powers, 2001) and distributing the estimated national emissions of mercury (34.49 short tons per year) across the 31 Mexican States and one Federal District weighting on a population basis. These emissions can be found in the following file:

arinv_nonpt_hg_mexico_all1999_fltmdl_21may2010_v4_ida.txt

A complete list of the names of the 2005 USEPA NEI emissions files (both original and updated) used as part of this project is included in Appendix C at the end of this document.

Methodology – Creation of CMAQ "Model-Ready" Emissions Files

The Sparse Matrix Operator Kernel Emissions (SMOKE) Modeling System (www.smoke-model.org) was used to convert "raw emissions input files" described above to a form that could be read directly into the CMAQ model. Separate processing runs were made for each of the

emissions categories: area, point, nonroad mobile, onroad mobile and biogenic. The processing was performed using a series of scripts and ancillary files, the latter of which were obtained from the USEPA Clearinghouse for Inventories & Emissions Factors (http://www.epa.gov/ttn/chief/). The basic steps to the emissions process include:

1. Raw emissions files for a given emissions category are read by SMOKE.
2. A series of ancillary files are called which control how SMOKE performs certain operations, including:
    - Determination of which pollutant species are to be processed for a given CMAQ Simulation.
    - Specification as to how to convert a given pollutant into its speciated members based upon emission source type (such as, waste incineration, electricity generation, etc.).
        - Ex: Converting total mercury into GEM, GOM and PBM
    - Application of temporal trends in anthropogenic emissions, including variations due to day of week, including holidays, and time of day.
    - Specification of land use category (ex: open soil, vegetation/type, water, etc.), including whether or not leaves are present on vegetation for a given time of year.
    - Determination of how processed emissions will be assigned to appropriate grid square for a given CMAQ modeling domain.

During the processing, the "raw emissions input files" described in the previous section where read by the SMOKE program and converted into hourly emissions for the final week of Calendar Year 2004, as well as the entirety of Calendar Year 2005. The biogenic emissions were generated within SMOKE, using the Biogenic Emission Inventory System (BEIS) v3.14. During this processing, the SMOKE program utilized the meteorological data generated by the WRF modeling effort, but in a modified format that was generated using the Meteorology-Chemistry Interface Processor (MCIP) which was obtained from the same location used to obtain the SMOKE model.

Following the generation of the sector specific emissions, these sectors were combined on an hourly basis to produced "merged" CMAQ "model-ready" emissions files that were read directly by CMAQ during the regional chemical simulations. The noted Calendar Year 2004 emissions were generated so that a one-week spin-up of the CMAQ model could be performed. The one week spin-up was performed, so that the chemical fields within the model would be at equilibrium with the emission/deposition processes prior to the start of the Calendar Year 2005 simulations. In this manner, emissions were generated for each of the three model grids utilized in this project (36km-, 12km- and 4km-gridcell domains).

Emissions Processing Results

Correction of Overestimation of Mercury Emissions from SMOKE Emissions Processing

During a quality assurance review of the emissions processing results at the end of the project, it was discovered that one of the original USEPA-provided raw emissions files was included in the processing, along with its updated version which had been updated using the information provided to the project team by the MDEQ. Inclusion of this original USEPA-provided raw emissions file resulted in an overestimate of emissions of mercury in the model for the entire Calendar Year 2005 BASE CASE model period. This overestimation of emissions subsequently impacted the modeled ambient concentrations and wet-/dry-deposition of mercury estimated during our CMAQ Model BASE CASE simulation.

Due to project deadlines, there was not an opportunity to re-run the SMOKE emissions processing and CMAQ model simulations for the entire year. However, based upon the linearity observed between mercury emissions and deposition (discussed below), we felt that it was possible to adjust both the ambient concentration data and the atmospheric deposition data generated by the model to correct for overestimation of mercury emissions. This adjustment was performed first by determining the ratio of "total mercury emissions without the extra file" to "total mercury emissions with the extra file" for each of our tagging categories. The ratios that were obtained are presented in Appendix B. Using these ratios, we scaled Calendar Year 2005 CMAQ Model BASE CASE simulation estimates to produce corrected values for the ambient concentrations of mercury, as well as the wet- and dry-deposition results from our CMAQ Model BASE CASE SIMULATION. While we understand that these adjustments are not tantamount to performing the entire year's emissions processing and CMAQ simulations, the project team feels that these adjustments provide an adequate correction of the data to allow us to provide guidance to the State of Michigan on:

- the spatial distribution of wet- and dry- deposition across the State of Michigan
- the relative impact of each tagging category to wet- and dry-deposition of mercury to the State of Michigan
- the relative impact of potential mercury emissions reductions within the State of Michigan

Emissions Summary

A series of "report files" were generated during the processing of emissions during the project. Using the original report files from the area, nonroad mobile and onroad model source sectors, and using the updated report files generated for the point source sector (without the extra emissions file described above), we were able to obtain a breakdown of the mercury emissions by county for the four anthropogenic source categories processed. The emissions attributed to each county for each sector can be found in Appendix B at the end of this report. A summary of the total mercury emissions in each of the four anthropogenic source categories is found in Table 10 below. As can be seen, following our update of the 2005 NEIv4.1 (based upon updates provided by the Michigan Department of Environmental Quality), our emissions estimates were

consistent with those of the full 2005 Michigan DEQ Mercury Inventory. While there were some differences with the Mobile Source emissions category, the overall total mercury emissions estimate (in tons per year, tpy) was quite close. As seen in Appendix B, the five Michigan counties with the largest emissions in our MI TMDL Calendar Year 2005 SMOKE Model BASE CASE SIMULATION were Monroe, Wayne, St. Clair, Alpena and Ottawa. Combined, these five counties contributed 50 percent of the total mercury emissions in the State of Michigan.

Table 10. Comparison of total mercury emissions (by sector) between the SMOKE MODEL BASE CASE simulation and the 2005 Michigan DEQ Mercury Emissions Inventory (MDEQ 2011).

FIPS	Point (tpy)	Area (tpy)	Onroad Mobile (tpy)	Nonroad Mobile (tpy)	Total (tpy)
Total Mercury Emissions	2.64	0.68	1.22E-02	7.79E-04	3.33
2005 Michigan DEQ Mercury Inventory	2.57	0.67	1.73E-04	2.57E-03	3.24

Additionally, as seen in Table 11, the total mercury emissions from the MI TMDL Calendar Year 2005 SMOKE Model BASE CASE simulation suggest that Michigan had some of the lowest emissions when compared with the surrounding states.

Table 11. Modeled emissions from Michigan and surrounding states from CMAQ Model BASE CASE simulation.

State	Total Hg Point (tpy)	Total Hg Area (tpy)	Total Hg Onroad (tpy)	Total Hg Nonroad (tpy)	Total Hg All Sectors (tpy)
Illinois	6.10	0.15	1.20E-02	5.07E-04	6.26
Indiana	5.41	0.10	7.80E-03	2.21E-04	5.52
Michigan	2.64	0.68	1.14E-02	1.16E-03	3.33
Ohio	5.72	0.16	1.23E-02	3.81E-04	5.89
Wisconsin	2.03	0.32	6.57E-03	7.82E-04	2.37

III. CMAQ Regional Chemistry Simulations

Methodology

Regional-scale photochemical simulations were performed using the Community Multi-scale Air Quality (CMAQ) model version 4.7.1, henceforth referred to as CMAQ. The CMAQ is the state-of-the-art model for analyzing photochemistry and transport of species in the atmosphere and for evaluating the impact of changes in emissions on air quality. CMAQ includes representations of the major photochemically active gas-phase species, including ozone, nitrogen oxides, an extensive representation of volatile organic compounds, and sulfur and other species relating to sulfate chemistry. It includes detailed representation of aqueous chemistry associated with formation of sulfates, and representation of the major particulate species, including trace metals.

These species provide the basis for representation of gas and aqueous chemistry of atmospheric mercury, including separate representation of gaseous elemental mercury (GEM), gaseous oxidized mercury (GOM) and particulate bound mercury (PBM). CMAQ methodology, results and model evaluations have been extensively described in peer-reviewed literature (Bullock 2002, 2008, 2009; Yu *et al*., 2010; Godowitch *et al*., 2011; and Appel *et al*., 2012)

CMAQ includes representation of each of the following atmospheric processes that affect ambient concentrations and deposition of mercury and other species:

- Emissions from anthropogenic and biogenic sources, based on a separate emissions model described above
- Vertical mixing within the daytime and nighttime boundary layers
- Horizontal advection and diffusion based on input meteorology from WRF
- Vertical advection associated with cloud formation, including separate representation of convective clouds
- Gas-phase photochemical transformations
- Aqueous phase photochemistry within cloud droplets
- Surface dry-deposition based on ambient concentrations and near-surface dynamics
- A one-dimensional soil model for dry-deposition and re-emission of mercury
- Wet-deposition based on calculated species concentrations within cloud droplets and rainfall rates.

Version 4.7.1, the most recent version at the time the modeling was conducted, is noteworthy because it included a one-dimensional representation of mercury in soils, including transport, storage and re-release to the atmosphere.

Processing of meteorological input from the WRF model (described above) was done using the MCIP Version 3.6.

For this project, two changes were made to the original CMAQ. These changes include the following:

(1) Changes relating to numerical methods, stability and error corrections:

These changes were developed at the University of Michigan based on experience with CMAQ Version 4.7 and 4.7.1 in order to prevent numerical crashes and (in one case) to correct an error with data processing. They should not affect the CMAQ science-based algorithms or substantive results. The changes are described in detail at the following web site:

http://www-personal.umich.edu/~sillman/CMAQ_corrections_2010.htm

(2) Changes to implement a "tagging" algorithm that tracks mercury from specified emission sources. This is described in detail below.

Model Application for Michigan TMDL:

The model application for Michigan consisted of three nested grids with horizontal resolution 36 km, 12 km and 4 km respectively, with advective transport from larger to smaller grids (Figure 1). As can be seen, the largest grid (36 km resolution) includes representation of the entire continental United States, plus parts of southern Canada and Northern Mexico. The 12 km grid includes representation of most of the eastern half of the U.S., including anthropogenic source regions in the Ohio River valley and urbanized regions of the northeast. The 4 km grid includes all of states of Michigan and Wisconsin, as well as the Chicago metropolitan area and emission sources in northern Indiana and Ohio that might impact Michigan.

Boundary conditions for the 36 km grid were set based on estimates for global background values, as shown below (Table 12).

Table 12. Boundary condition values for the 36km Grid of our CMAQ MODEL BASE CASE simulation are given for model sigma altitudes 0.99, 0.95, 0.88, 0.72, 0.45, and 0.15, corresponding approximately to 990, 950, 880, 720, 450 and 150 hPa (millibars), respectively, for a column of air at sea level. All species not included in the table have boundary values equal to zero.

		Sigma Altitude					
Mercury species	**units**	**0.99**	**0.95**	**0.88**	**0.72**	**0.45**	**0.15**
HG	ppb	1.78E-04	1.77E-04	1.76E-04	1.75E-04	1.74E-04	1.73E-04
RGM	ppb	2.00E-06	3.00E-06	4.00E-06	5.00E-06	6.00E-06	7.00E-06
HgP	ug m^{-3}	1.08E-05	1.03E-05	9.72E-06	7.56E-06	4.86E-06	1.62E-06
Other gas-phase species							
SO2	ppb	3.00E-01	2.00E-01	1.00E-01	1.00E-04	2.00E-02	1.00E-02
NO2	ppb	1.67E-01	1.67E-01	8.40E-02	0.00E+00	0.00E+00	0.00E+00
NO	ppb	8.30E-02	8.30E-02	4.20E-02	0.00E+00	0.00E+00	0.00E+00
O3	ppb	3.50E+01	3.50E+01	4.00E+01	5.00E+01	6.00E+01	7.00E+01
HNO3	ppb	5.00E-02	5.00E-02	5.00E-02	5.00E-02	7.00E-02	1.00E-01
H2O2	ppb	1.00E+00	1.00E+00	1.50E+00	1.00E+00	8.00E-01	2.00E-01
ALD	ppb	3.00E-02	3.50E-02	3.00E-02	2.00E-02	2.00E-02	1.00E-02
HCHO	ppb	2.50E-01	2.50E-01	2.50E-01	2.00E-01	1.00E-01	5.00E-02
NH3	ppb	1.00E-01	1.00E-01	3.00E-02	2.00E-02	2.00E-02	1.00E-02
PAN	ppb	1.00E-01	1.00E-01	5.00E-02	5.00E-02	1.50E-02	0.00E+00
HC3	ppb	4.00E-02	4.00E-02	3.20E-02	1.20E-02	4.00E-03	0.00E+00
HC5	ppb	4.00E-02	4.00E-02	3.20E-02	1.20E-02	4.00E-03	0.00E+00
HC8	ppb	2.00E-02	2.00E-02	1.60E-02	6.00E-03	2.00E-03	0.00E+00
ETH	ppb	1.00E-01	1.00E-01	8.00E-02	3.00E-02	1.00E-02	0.00E+00
CO	ppb	8.00E+01	8.00E+01	8.00E+01	7.00E+01	6.50E+01	5.00E+01
OL2	ppb	5.00E-03	3.00E-03	2.00E-03	1.00E-03	1.00E-03	0.00E+00
OLT	ppb	2.00E-04	2.00E-04	1.00E-04	0.00E+00	0.00E+00	0.00E+00
OLI	ppb	1.00E-04	1.00E-04	0.00E+00	0.00E+00	0.00E+00	0.00E+00
TOL	ppb	1.00E-03	1.00E-03	1.00E-03	1.00E-03	0.00E+00	0.00E+00
XYL	ppb	2.00E-04	2.00E-04	1.00E-04	0.00E+00	0.00E+00	0.00E+00
ACO3	ppb	1.00E-06	1.00E-06	1.00E-06	1.00E-06	1.00E-06	1.00E-06
TPAN	ppb	1.00E-05	1.00E-05	1.00E-05	1.00E-05	1.00E-05	1.00E-05
HONO	ppb	1.00E-06	1.00E-06	1.00E-06	1.00E-06	1.00E-06	1.00E-06
HNO4	ppb	2.00E-06	2.00E-06	2.00E-06	2.00E-06	2.00E-06	2.00E-06
KET	ppb	5.00E-01	5.00E-01	5.00E-01	3.33E-01	3.33E-01	1.67E-01
GLY	ppb	2.50E-04	2.50E-04	2.50E-04	2.00E-04	1.00E-04	5.00E-05
MGLY	ppb	2.50E-04	2.50E-04	2.50E-04	2.00E-04	1.00E-04	5.00E-05
DCB	ppb	2.50E-04	2.50E-04	2.50E-04	2.00E-04	1.00E-04	5.00E-05
ONIT	ppb	2.00E-02	2.00E-02	1.60E-02	6.00E-03	2.00E-03	0.00E+00
ISO	ppb	1.50E-01	1.50E-01	0.00E+00	0.00E+00	0.00E+00	0.00E+00
MACR	ppb	1.50E-02	1.50E-02	0.00E+00	0.00E+00	0.00E+00	0.00E+00
MVK	ppb	3.00E-02	3.00E-02	0.00E+00	0.00E+00	0.00E+00	0.00E+00
BENZENE	ppb	4.45E-02	4.45E-02	4.45E-02	3.89E-02	3.62E-02	2.78E-02

Table 12 (Continued)

		Sigma Altitude					
Aerosol species	**units**	**0.99**	**0.95**	**0.88**	**0.72**	**0.45**	**0.15**
ASO4I	ug m^{-3}	4.81E-03	4.81E-03	3.21E-03	3.21E-03	6.41E-04	3.21E-04
ASO4J	ug m^{-3}	5.96E-01	5.96E-01	3.98E-01	3.98E-01	7.95E-02	3.98E-02
ASOIL	ug m^{-3}	2.15E-01	1.83E-01	1.21E-01	5.40E-02	1.34E-02	1.34E-02
ACORS	ug m^{-3}	3.39E-01	2.89E-01	1.90E-01	8.51E-02	2.11E-02	2.11E-02
NUMCOR	ug m^{-3}	2.35E+04	1.63E+04	6.34E+03	1.16E+03	2.03E+02	2.00E+02
ANIJ	ug m^{-3}	9.51E-05	8.09E-05	5.33E-05	2.39E-05	5.91E-06	5.91E-06
ACR_IIIJ	ug m^{-3}	7.50E-06	6.38E-06	4.21E-06	1.88E-06	4.66E-07	4.66E-07
ACR_VIJ	ug m^{-3}	7.50E-06	6.38E-06	4.21E-06	1.88E-06	4.66E-07	4.66E-07
APBJ	ug m^{-3}	1.41E-05	1.20E-05	7.90E-06	3.54E-06	8.76E-07	8.76E-07
APBK	ug m^{-3}	9.39E-06	7.99E-06	5.27E-06	2.36E-06	5.84E-07	5.84E-07
ACDJ	ug m^{-3}	1.76E-06	1.50E-06	9.87E-07	4.42E-07	1.10E-07	1.10E-07
AMNJ	ug m^{-3}	9.39E-05	7.99E-05	5.27E-05	2.36E-05	5.84E-06	5.84E-06
AMNK	ug m^{-3}	1.41E-04	1.20E-04	7.90E-05	3.54E-05	8.76E-06	8.76E-06
AALKJ	ug m^{-3}	2.80E-03	2.28E-03	1.32E-03	4.92E-04	2.22E-05	2.78E-08
AXYL1J	ug m^{-3}	6.00E-04	4.89E-04	2.83E-04	1.05E-04	4.77E-06	5.95E-09
AXYL2J	ug m^{-3}	2.00E-04	1.63E-04	9.42E-05	3.51E-05	1.59E-06	1.99E-09

For the purpose of the TMDL simulation the most important boundary conditions are those for mercury species. GEM is particularly important because it has a long lifetime in the atmosphere (approximately one year), so that its presence in a regional simulation is largely determined by the boundary assumption. We assume a background concentration for GEM at the surface of 1.4 ng m^{-3} (which is the default value used in CMAQ) and its equivalent (adjusted for atmospheric pressure and density) at higher altitudes. Background concentrations of GOM and PBM are somewhat less important, because these species are likely to be deposited relatively quickly and regenerated from emissions and chemistry within the model domain, rather than impacting Michigan directly. We assume 16 pg m^{-3} GOM at the surface, increasing to 48 pg m^{-3} at 500 mb. Background PBM Hg is 10 pg m^{-3} at the surface and decreasing with altitude. These boundary concentrations insure that deposition of mercury from background sources in Michigan is not underestimated, and may tend to be overestimated by up to 20 percent.

Two other changes in parameters from the standard CMAQ 4.7.1 settings were made:

Soil concentrations of mercury for the 1d soil model were set at 50 ng/g, rather than the CMAQ default setting of 90 ng/g, based on reported measurements (Zhang *et al.*, 2001; Ericksen *et al.*, 2006).

An oxidation reaction between GEM and NO3 (GEM+NO3=>NO2) was removed from the gas-phase chemistry, based on recommendations from the creators of CMAQ (J. Bash, EPA ORD, personal communication, 12-19-10). The NO3 reaction is usually not included in models for the chemistry of mercury and is expected to be omitted from future versions of CMAQ.

Tagging, Linearity and sensitivity to precursor emissions

CMAQ Version 4.7.1 has been modified at the University of Michigan to include a tagging method for representing mercury from specific sources and tracking source-based mercury throughout all atmospheric processes represented in the simulation. The tagging representation provides the basis for determining Hg deposition within the model for scenarios with different emission rates from the CMAQ Model BASE CASE. This includes corrections to emission rates used in the model initial scenario in order to include the most recent representation of 2005 emissions. Tagging is also used to determine predicted responses to proposed changes in emission rates. The following section describes the tagging method, the rationale for using tagging to represent changes in emissions, and testing of the model with tagging to verify that emissions changes are represented properly.

Concept:

Tagging involves the addition of sub-species to the model calculation (tagged species) that are identical to the original or base species, but represent only the part of the species with a specific origin or emissions source. Tagged species concentrations are then calculated in an identical way as the base species, including all model processes: emissions, advection, diffusion, photochemical transformation, and removal through deposition. The only difference between the tagged species calculation and that of the base species is that the tagged species source (either as emissions or transport from outside the model boundary) is limited to a subset of all sources that are included in the base species. Other sources are set to zero in the tagged species calculation. For example: a tagged species might represent emissions from coal-fired power plants in one state, in which case emissions from all other sources, from other states and other countries are all set to zero and boundary conditions for the largest model domain are set to zero. The calculation of the tagged species is identical to the base species for all other processes represented in the CMAQ Model BASE CASE. Tagged species can be advected from larger model domains to sub-domains, in the same manner as the base species. It is also possible to represent transport from outside the model boundary by a tagged species, by setting the boundary condition for the tagged species equal to that of the base species and setting all emissions equal to zero for the tagged species.

Tagging (or tracer species) has been used before in investigations of global transport and photochemistry (Wang *et al*., 1998, Li *et al*., 2002; Fiore *et al*., 2002). It has also been used in the REMSAD model for mercury.

In theory, the tagged species represent the precise amount of the base species that originated from the tagged species source at any point in the model calculation (including ambient concentrations, wet- or dry-deposition at any specific time or model location). This is true subject to two conditions (chemistry and completeness of the model representation), described below.

A central question is whether this type of tagging can also be used to represent model wet- and dry-deposition for emissions scenarios that differ from the model base case, including scenarios for the model predicted response to changes in emissions. This question is closely connected to the question of ***linearity*** in model responses. If the model responds in a linear way to changes in emissions, then the tagged species can also be used to calculate the model response to emissions changes. The response is calculated by applying the desired percent change in emission rates to the amount of tagged species in the model at any specific time or location. To take a specific example: if the tagged mercury wet-deposition from non-specified emissions sources from the State of Michigan was 12 $\mu g/m^2$ in the model for Detroit during the month of July, then a 33 percent reduction in emissions from those sources would result in a 4 $\mu g/ m^2$ reduction in wet-deposition.

The response to changes in precursor emissions is often not linear for many chemically active atmospheric pollutants. Ozone shows a strongly nonlinear response to changes in emissions of its main precursors, NO_x and VOC. Deposition of nitrate and sulfate aerosols also show somewhat of a nonlinear response. The nonlinear effects occur primarily because the process of formation of ozone, nitrates and sulfates (and concurrent removal of precursor species NO, NO_2 and SO_2) also causes changes in other species that affect the rate of formation. These other species are the OH radical and (in the case of sulfate) aqueous H_2O_2. The chemistry of mercury is different because mercury is a trace species, so that the reactions associated with mercury are usually too slow to have much effect on other species. Because other species are largely unaffected by changes in mercury concentrations, the rates of photochemical processing of mercury are directly proportional to the amount of mercury in the atmosphere.

The tagging method for mercury has been tested both for linearity and for the response to changed emissions in comparison with model scenarios with different emissions, as described below.

Tagging and model chemistry:

Photochemical transformations associated for tagged species for mercury were represented as follows. For each emission source, a separate tagged species was used to represent three classes of atmospheric mercury: GEM, GOM, and PBM (representing the sum of three particulate mercury species included in CMAQ).

Photochemistry (both gas and aqueous) was calculated for the original ensemble of model species as in the standard CMAQ, with the original full mercury species representing mercury. The rates of photochemical transformation between GEM, GOM, and PBM and removal rates of each mercury species in the full solution were then used to calculate transformations of the tagged species. Transformations for the tagged species were represented as transformations between species with the same tag (tagged GEM to tagged GOM, etc.). We used a reverse-Euler solution for the individual tagged species, which provided a stable solution for rapidly interacting species. One noteworthy feature is that the impact of reactions involving mercury on other non-mercury species only occurs through the original model mercury species, which are identical to the original CMAQ. The tagged species have no effect on non-mercury species or on mercury species with different tags in the calculation.

Completeness of model representation:

The ensemble of model tags has been chosen to include representation of mercury from all sources in the model. This includes all non-specified emission sources, initial concentrations within the model domain at the start of the simulation and transport from outside the model domain.

The complete model representation provides an important test for quality assurance. The model includes the original CMAQ Model BASE CASE calculations for ambient concentration and deposition of mercury along with the equivalent for a complete set of tags. If tags in the model have been implemented correctly, then the sum over all the tags should be equal to the equivalent model value for the original species.

Tagged species included in simulations for MI-TMDL:

Tags include the following:

1. MIEC: Coal-fired electricity generation in the State of Michigan
2. MIIN: Waste incinerators in the State of Michigan
3. MIMET: Steel manufacturing in the State of Michigan
4. MICM: Cement kilns within Michigan
5. MI: All other anthropogenic emission sources in Michigan
6. OH: Ohio, all sources.
7. IN: Indiana, all sources.
8. IL: Illinois, all sources.
9. WI: Wisconsin, all sources.
10. MN: Minnesota, all sources.
11. US: All sources in the US outside of the states included above.
12. Misc: All remaining emission sources, including Canada and Mexico.
13. SOIL: Soil emissions.
14. BNDY: Transport from outside the boundary of the largest model domain, and initial mercury content at the start of the simulation.

In reporting the final results, the SOIL tag has been removed and the amount distributed among all other sources in proportion to the amount already contained in the equivalent tag. This is because CMAQ includes rapid exchange between the atmosphere and soil, so that the soil tag effectively represents an ensemble of all other tags for each location.

Evaluation of tagging representation:

The tagging representation has already been extensively evaluated in the application of CMAQ for the State of Florida as part of the Florida Mercury TMDL. The evaluation included three components.

1. Conservation of mass: comparison between the original simulation result for Hg wet deposition, dry deposition and species concentrations and the equivalent sum of tagged species, to insure that differences are no more than 2 percent.

2. Test for linearity: comparison of changes between simulations for the base case scenario and (a) simulations with 50 percent reductions in emissions from all anthropogenic sources in the state of Florida; and (b) simulations with 99 percent reductions in the state of Florida. A linear response implies reductions in deposition (as determined by the difference between the base case and the reduction scenario) should be greater for the 99 percent relative to 50 percent reductions, by a factor of nearly double (1.99).

3. Test for tagging and emissions: comparison of changes in deposition between simulations for the base case and reduced-emissions scenarios from the estimates for changes derived from tagging. The tagging estimates are derived by assuming that the tagged mercury from each emissions source represents the change that would result from a 100 percent reduction in emissions from that source, and that changes from smaller percent reductions are smaller by the specified percentage. Tests for Florida involved models with 50 percent and 99 percent reductions in emissions from all anthropogenic sources in the state for the months of January, May and July.

For Michigan, we have performed the following tests to evaluate tagging:

1. Conservation of mass: comparisons between the original simulation result for Hg wet deposition, dry deposition and species concentrations and the equivalent sum of tagged species.

2. Tagging and emissions: evaluation of the change in Hg between a model base case scenario and a scenario with 90 percent reductions in emissions from all coal-fired power plants (EGUs) in the State of Michigan, compared to the estimated change from tags for emission sources in the base case.

Results for the conservation of mass test are shown in Figures 3 and 4. Results for the tagging and emissions test are shown in Figures 5-8. Results are shown for two months (January and July) and represent comparisons for each day of the month.

As can be seen, there is a near-exact correspondence between the model deposition and the sum of tags. There is a close correspondence between the model reduction in deposition associated with a 90 percent reduction in emissions from coal-fired EGUs and the reduction in deposition derived from tags rather than from a separate simulation.

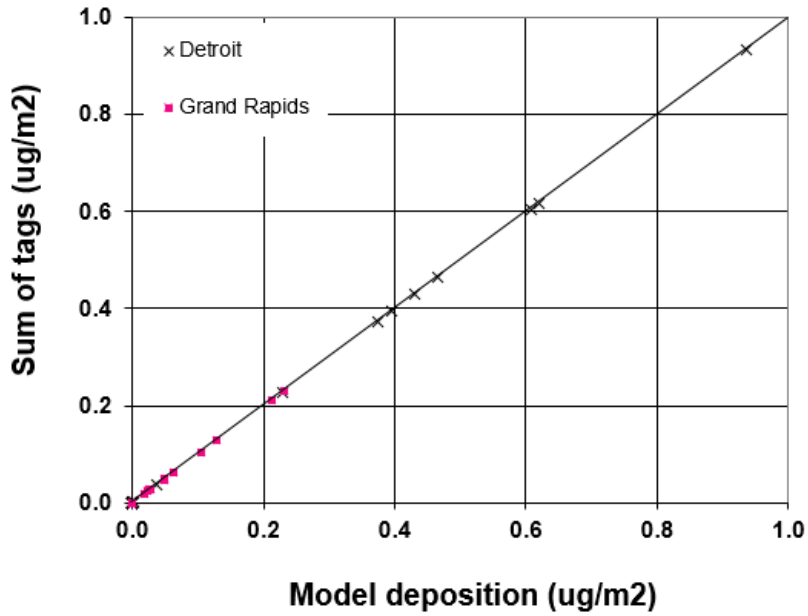

(a) January

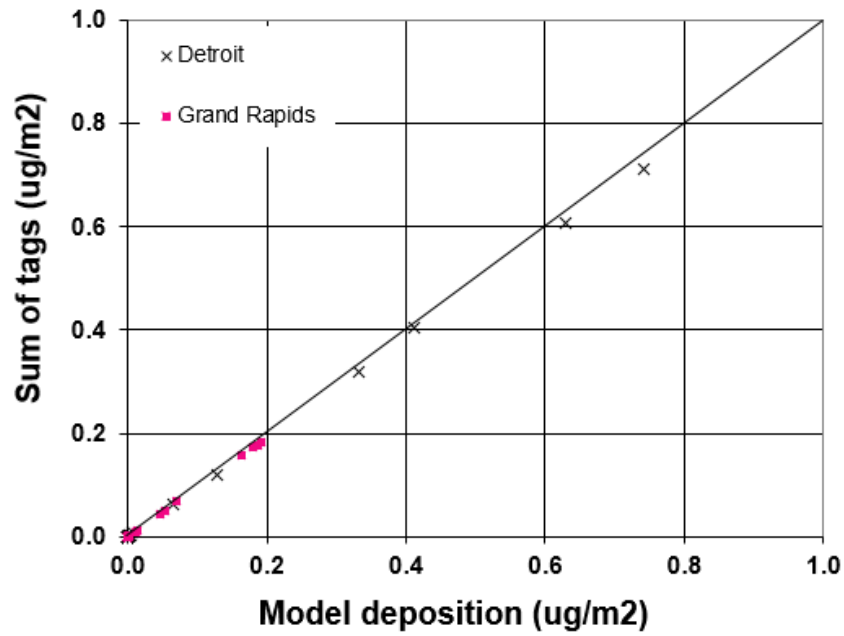

(b) July

Figure 3. Model day-by-day wet deposition of mercury (µg/m^2) at Detroit (X's) and Grand Rapids (red squares) for (a) January and (b) July, comparing the direct deposition in the model for each day with the equivalent sum of deposition of model tagged species (conservation of mass test).

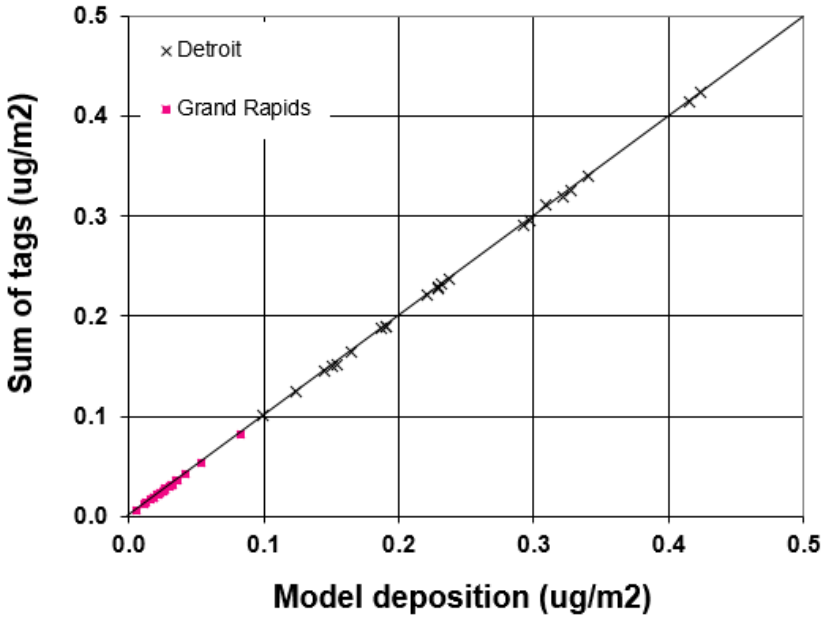

(a) January

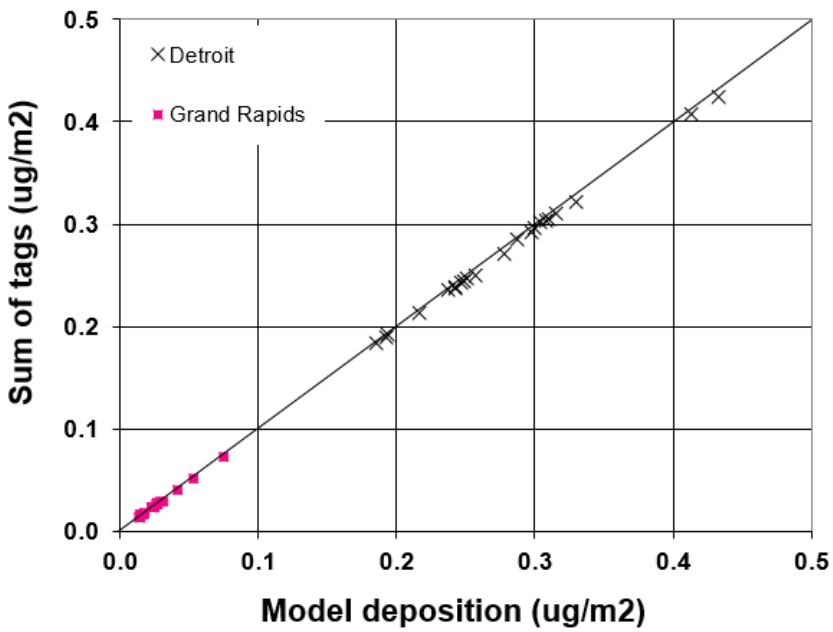

(b) July

Figure 4. Model day-by-day dry deposition of mercury (µg/m^2) at Detroit (X's) and Grand Rapids (red squares) for (a) January and (b) July, comparing the direct deposition in the model for each day with the equivalent sum of deposition of model tagged species (conservation of mass test).

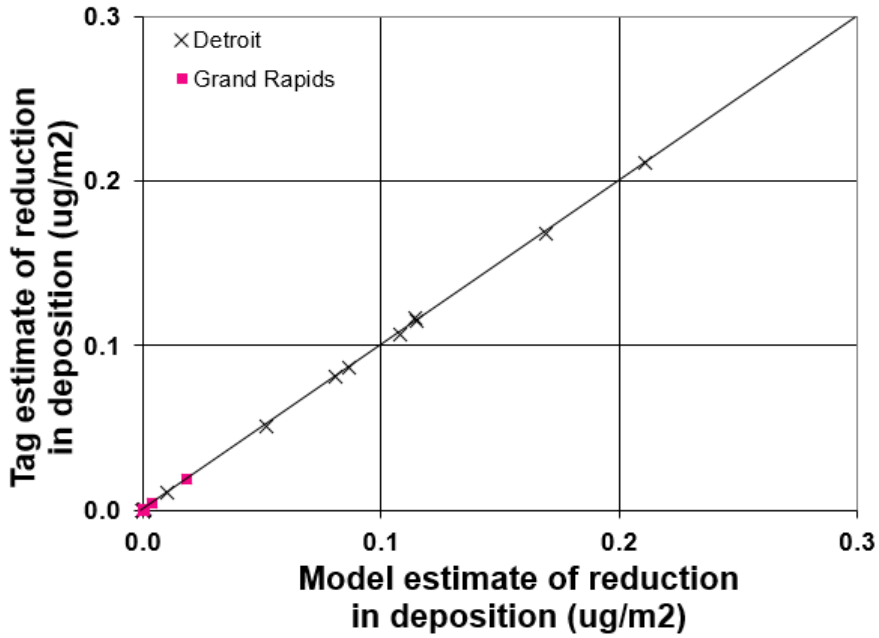

(a) January

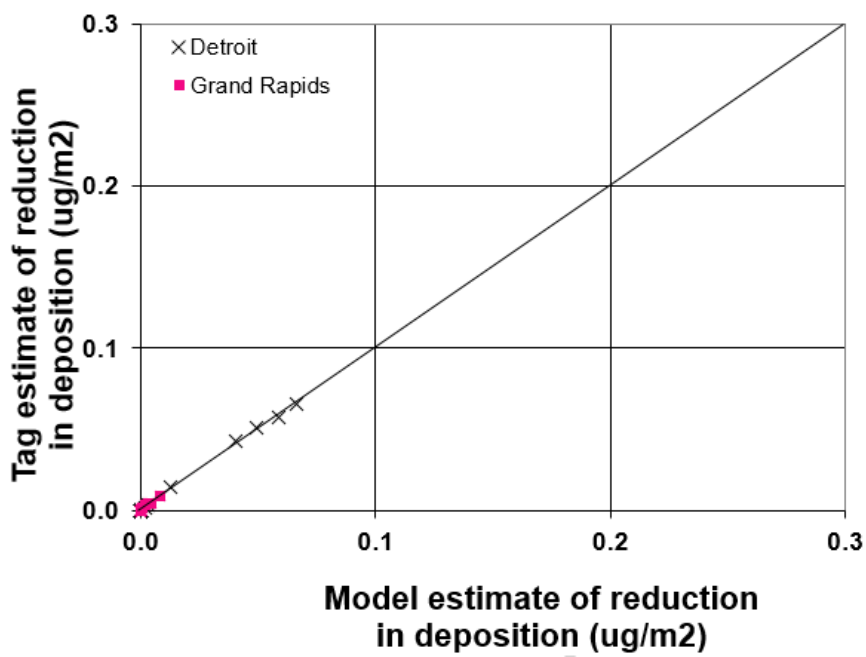

(b) July

Figure 5. Model reduction in wet deposition of mercury (µg/m^2) at Detroit (X's) and Grand Rapids (red squares) for (a) January and (b) July, resulting from a 90 percent reduction of emissions from coal-fired power plants in the State of Michigan. The plot compares the day-by-day reduction in deposition determined as the difference between model base case and reduced emissions scenarios (horizontal axis) with the reduction derived from model tags in the base case (vertical axis).

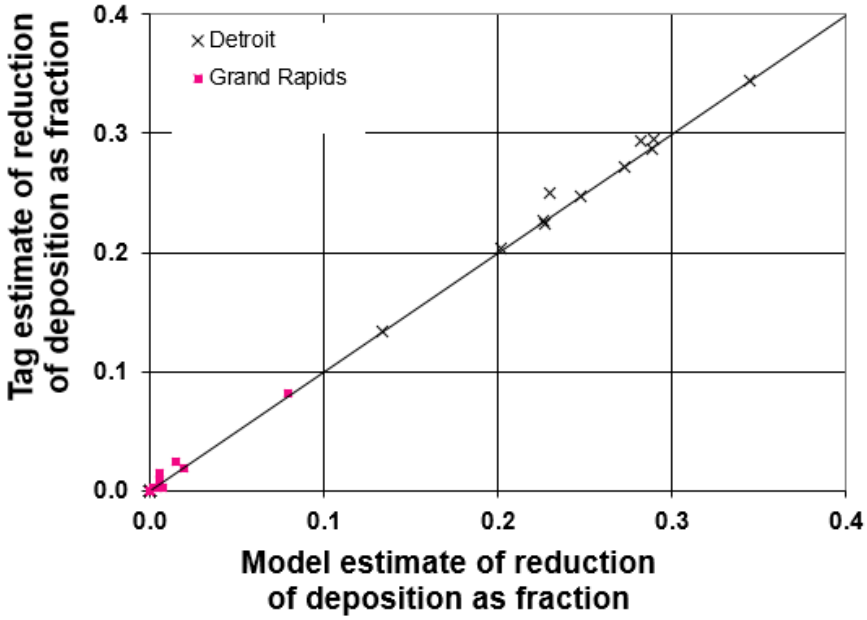

(a) January

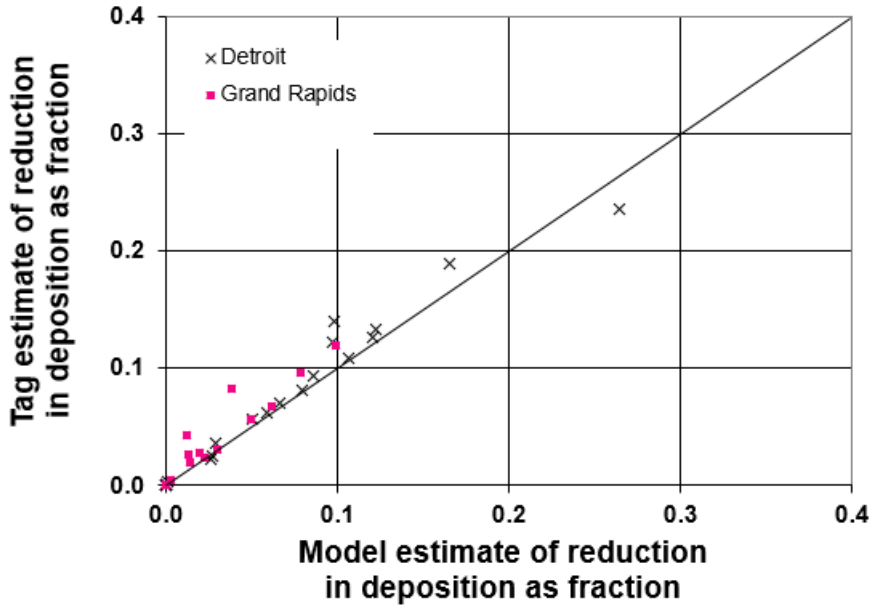

(b) July

Figure 6. Model reduction in wet deposition of mercury as a fraction of total mercury wet deposition at Detroit (X's) and Grand Rapids (red squares) for (a) January and (b) July, resulting from a 90 percent reduction of emissions from coal-fired power plants in the State of Michigan. The plot compares the day-by-day reduction in deposition determined as the difference between model base case and reduced emissions scenarios (horizontal axis) with the reduction derived from model tags in the base case (vertical axis).

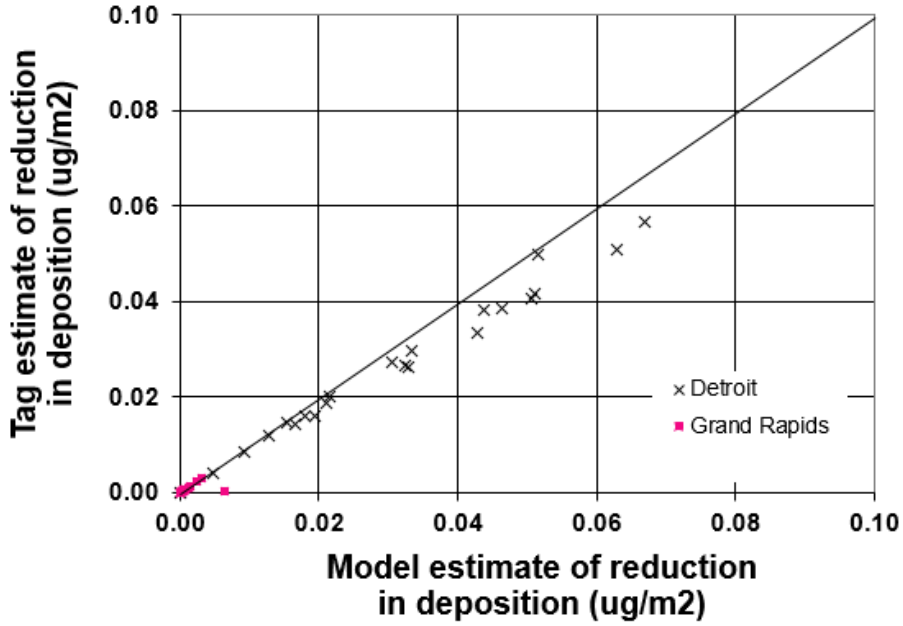

(a) January

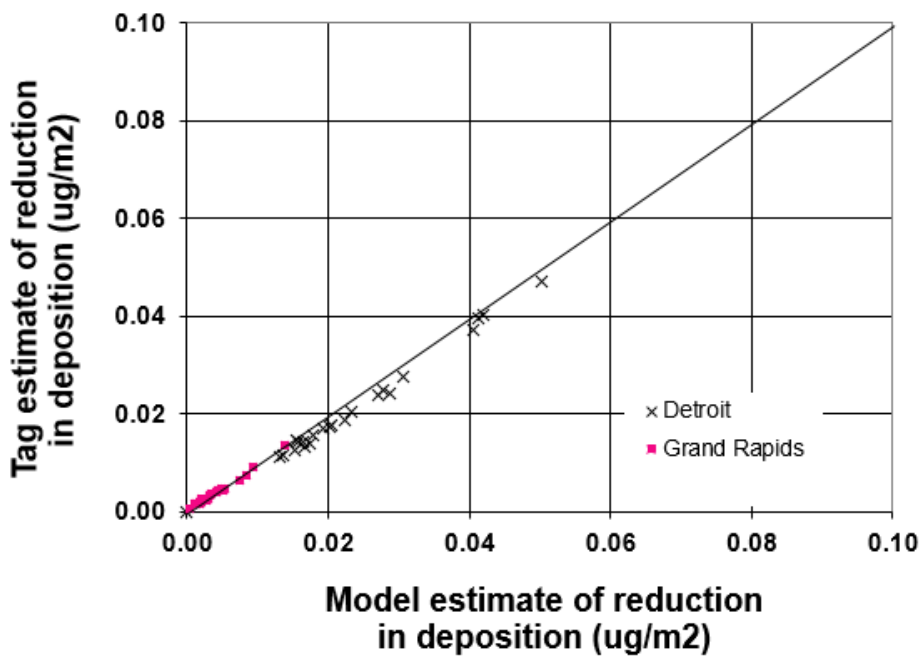

(b) July

Figure 7. Model reduction in dry deposition of mercury (µg/m^2) at Detroit (X's) and Grand Rapids (red squares) for (a) January and (b) July, resulting from a 90 percent reduction of emissions from coal-fired power plants in the State of Michigan. The plot compares the day-by-day reduction in deposition determined as the difference between model base case and reduced emissions scenarios (horizontal axis) with the reduction derived from model tags in the base case (vertical axis).

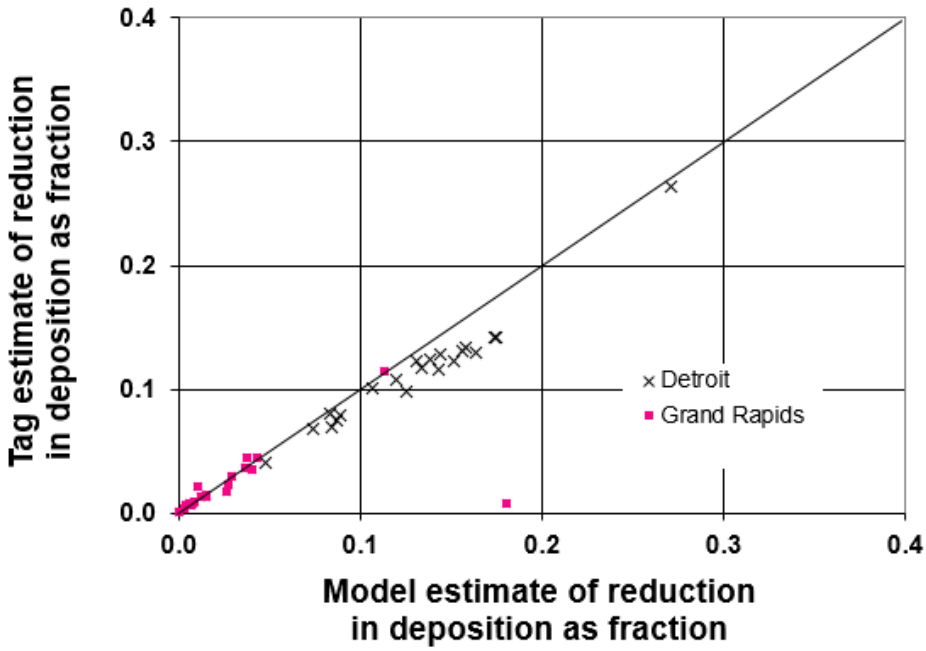

(a) January

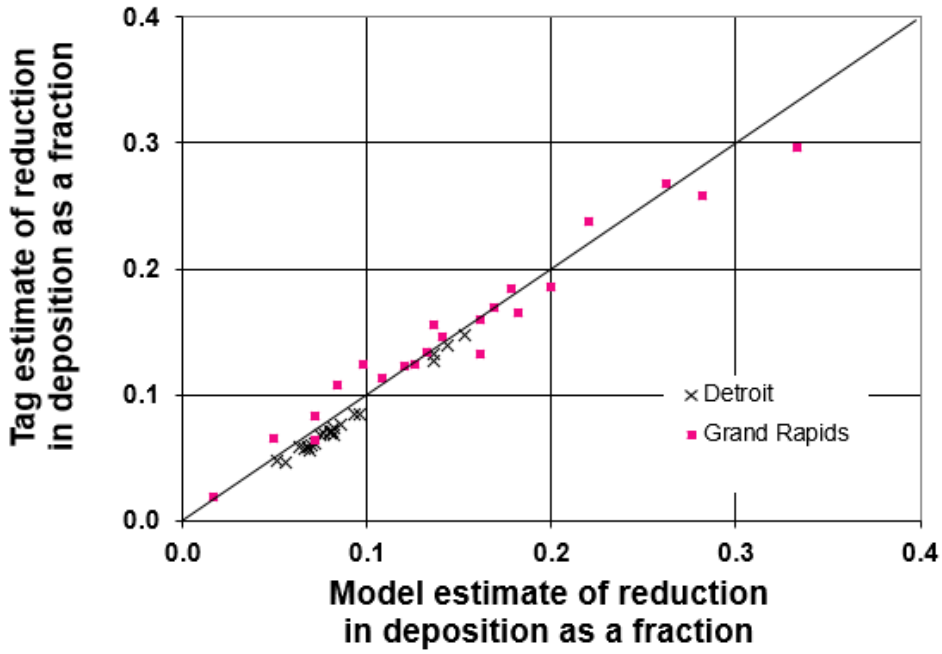

(b) July

Figure 8. Model reduction in dry deposition of mercury as a fraction of total mercury wet deposition at Detroit (X's) and Grand Rapids (red squares) for (a) January and (b) July, resulting from a 90 percent reduction of emissions from coal-fired power plants in the State of Michigan. The plot compares the day-by-day reduction in deposition determined as the difference between model base case and reduced emissions scenarios (horizontal axis) with the reduction derived from model tags in the base case (vertical axis).

CMAQ MODEL BASE CASE Simulation Results

CMAQ estimates of total mercury deposition, both wet- and dry-, for Calendar Year 2005 are presented for several locations across the State of Michigan in Figure 9. The highest deposition totals were predicted for the Detroit metropolitan area (here represented by the location of the MDEQ Livernois sampling site) and Flint. For both the Detroit (Livernois) and Flint sites, the CMAQ Model BASE CASE simulation suggests that dry-deposition exceeded wet-deposition, with dry-deposition estimated to be twice the wet-deposition flux at Flint. It is not surprising that the predicted deposition in the Detroit area exceeds that of most other sites, as the three counties with the highest total mercury emissions are within the Detroit area (Monroe, Wayne and St. Clair counties). This proximity to local, anthropogenic emissions is likely the reason that dry-deposition exceeds wet-deposition at the site, given that the conventional wisdom is that both GOM and PBM are deposited near sources, in part due to their reactivity relative to GEM. It is interesting that the Flint site was predicted to have such elevated dry-deposition, given that Kent (Grand Rapids) and Washtenaw (Dexter) Counties have similar total mercury emissions to Genesee County (Flint). While this may be related to the relative speciation of mercury emissions within those counties, a more likely explanation is related to the location used for our Flint receptor site. The site chosen was in close proximity to the gridded emissions used in our modeling effort. It is common for gridded models to produce elevated deposition estimates for receptor locations within or next to the model grid cells with anthropogenic emissions due to the fact that that emissions within model grid cells are instantly dispersed across the entire grid cell resulting in strong deposition to that, or adjoining, grid cells. In reality, emissions may stay aloft within elevated plumes and deposited farther downwind.

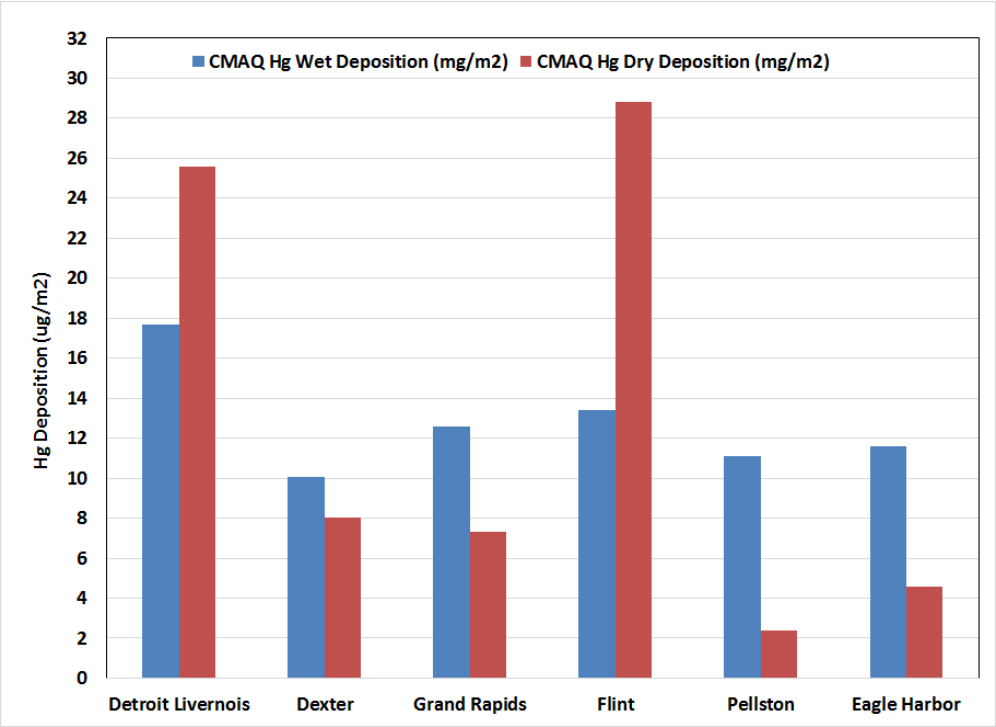

Figure 9. Summed annual (2005) CMAQ Model BASE CASE simulation Mercury Wet- and Dry-deposition (µg/m^2) at a select series of locations across the State of Michigan.

Overall, these deposition estimates are quite consistent with those generated by the Regional Modeling System for Aerosols and Deposition (REMSAD) model that was used in the preparation of the Statewide Michigan Mercury TMDL (LimnoTech, 2013), as presented in Figure 10. The estimates obtained using the REMSAD model were performed using the USEPA 2001 National Emissions Inventory. The USEPA 2001 National Emissions Inventory estimated total mercury emissions from the State of Michigan to be approximately 3.6 tons, which was slightly greater than the 3.3 tons utilized in our BASE CASE simulation (LimnoTech, 2013). A breakdown of the relative contribution of wet- and dry-deposition at each site was not available for the REMSAD simulations.

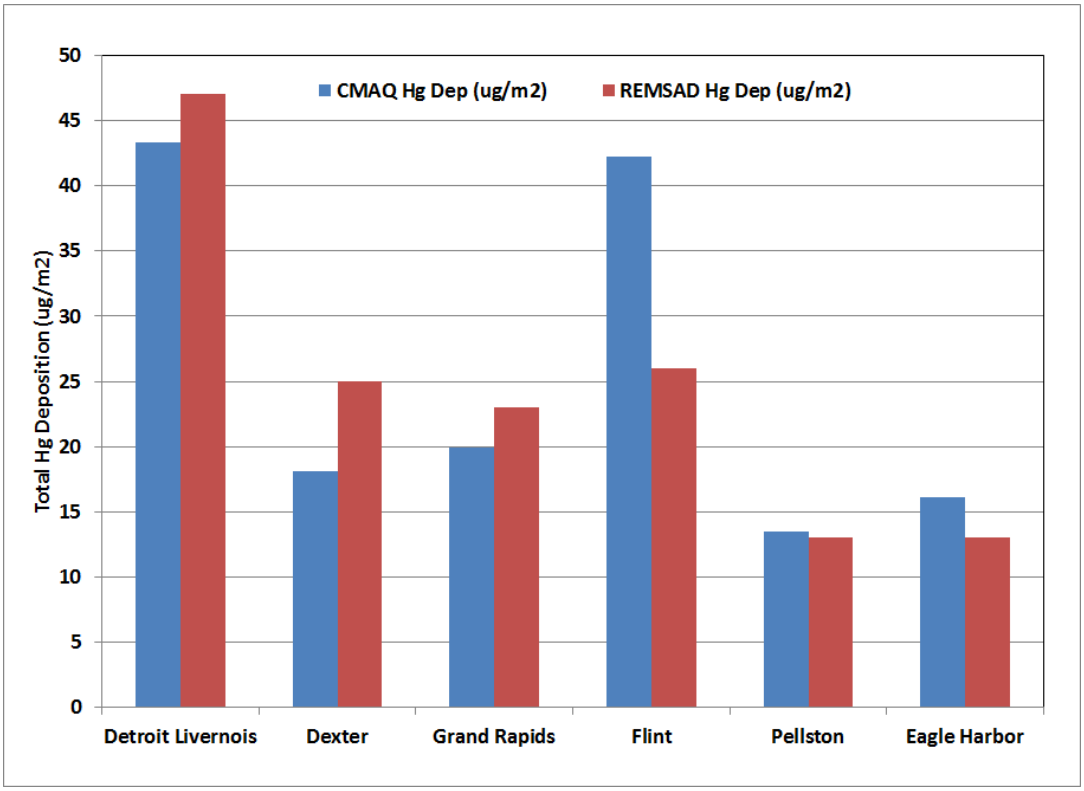

Figure 10. Summed annual (2005) Total Mercury (Wet- + Dry-deposition (µg/m^2)) from 2005 CMAQ Model BASE CASE and 2001 REMSAD simulations at a select series of locations across the State of Michigan.

Measurement Model Comparison: Ambient Speciated Concentrations

A summary of the comparison between the ambient speciated mercury measurements performed by the University of Michigan Air Quality Laboratory (UMAQL) and the CMAQ Model BASE CASE simulations are presented in the tables within Appendix C. Both the measurements and simulations are for Calendar Year 2005. The measurements are from the UMAQL's Detroit/Fort Street and Dexter, Michigan sites. As noted earlier, the CMAQ Model BASE CASE simulation data is for a location close to the MDEQ Livernois monitoring site and the UMAQL's Dexter, Michigan site. The CMAQ Model BASE CASE simulation output for a location close to the MDEQ Livernois site was used in place of model output at the location of the Fort Street site,

given that we felt that the model significantly over-predicted deposition for the Fort Street site given that it was so close to emissions sources. This over prediction is often seen in other regional chemical models (such as REMSAD) given the manner in which the model spread emissions instantly across a given grid box.

The data used to compute the statistical measures presented in the tables within Appendix C were daily average values. For both the Detroit (Livernois) and Dexter site, the monthly Pearson correlation coefficients varied between negative and positive values for GEM, while the monthly Pearson correlation coefficients for GOM and PBM were generally positive. A more consistent picture appears when one considers the measure "mean error". In this measure, it can be seen that the CMAQ Model BASE CASE simulation results show a consistent under-prediction of GEM and a consistent over-prediction of GOM and PBM, though this trend is more pronounced at the Detroit site. Without additional field measurements, it is difficult to pinpoint the cause of this observed trend. For example, it is possible that the results are suggesting that CMAQ Model BASE CASE simulation converted too much GEM to GOM on a short timescale and thus close to the source locations within the model. Additionally, it is possible that the standard speciation values within the 2005 USEPA NEIv4.1 used in the study partition too low of a percentage of total mercury to GEM and too high of a percentage to GOM and PBM.

Though the magnitudes of the errors vary from month to month, the trends regarding under-prediction and over-prediction are consistent. Given that GOM and PBM are typically deposited in the near field, this tendency would likely cause the model to over-predict the levels of both wet- and dry-deposition in the near field surrounding sources. It should be noted that due to instrument difficulties at the Dexter site, 19 of 31 days of measured ambient concentration data were missing during the month of July 2005 and 24 of 31 days of measured ambient concentration were missing during the month of December 2005.

Measurement Model Comparison: Wet Deposition

As part of our evaluation of the CMAQ Model BASE CASE simulation performance, we compared the mercury wet-deposition measurements from the Michigan Mercury Network for several sites for Calendar Year 2005 against the mercury wet-deposition predicted for those same sites by our CMAQ Model BASE CASE simulation for the same period. As can be seen in Figure 11, the CMAQ Model BASE CASE simulation was able to predict the overall magnitude and geographic variations in the observed mercury wet-deposition. While the mercury wet-deposition to the Dexter and Grand Rapids sites were predicted to within 10 to 20 percent (over predictions), the difference between the measured mercury wet-deposition and the CMAQ Model BASE CASE simulation predictions were greater for both Pellston and Eagle Harbor. These differences are consistent with the larger over-prediction of precipitation at the Pellston and Eagle Harbor sites by the WRF model, as discussed in an earlier part of this report.

Performance statistics for the wet-deposition evaluations, based on monthly values at each site over the Calendar Year 2005, resulted in a normalized mean bias of 40 percent, and normalized mean error of 79 percent. These performance values are very similar and quite typical of other

previous studies. For example, Bullock *et al*. (2009) reported performance statistics for three different urban/regional-scale models (including CMAQ) combined with three different global-scale models, for a total of nine comparisons. They evaluated results for a one-year simulation for 2001 in comparison with weekly measurements of wet deposition and precipitation from the MDN network of 62 sites located throughout the U.S. (mostly in the eastern half).

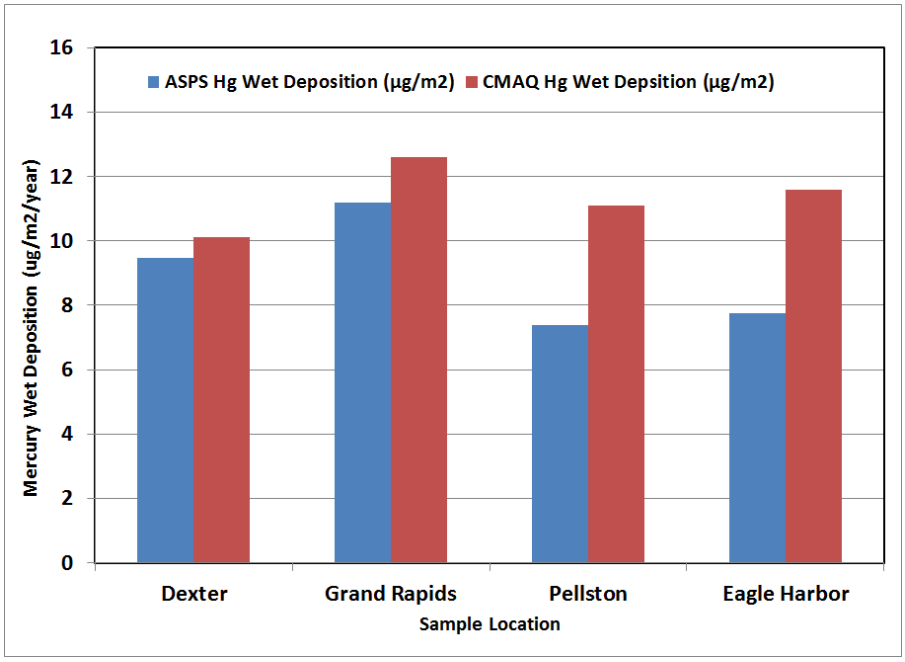

Figure 11. Comparison of mercury wet-deposition measured by the Michigan Mercury Network and mercury wet-deposition predicted by the CMAQ Model BASE CASE simulation. Each represents the annual total for Calendar Year 2005.

They found normalized mean bias for the various model combinations ranging from -50 percent to +87 percent. There was significant variation between the three urban/regional models. In their study, CMAQ had relatively low mean bias, with values from -50 percent to +16 percent depending on the global background model, while the REMSAD model tended to over-predict somewhat, with mean bias from +16 percent to +40 percent. The third regional model, TEAM, showed a major over-prediction with mean bias +62 percent to +87 percent. Normalized mean errors were 71 percent to 85 percent (CMAQ), 82 percent to 90 percent (REMSAD) and 105 percent to 130 percent (TEAM). Coefficients of determination (r^2) were relatively low for all models, ranging from 0.12 to 0.18. The relatively high mean errors and low coefficients of determination were driven largely by differences between the model and observed weekly precipitation (normalized mean error 62 percent, $r^2 = 0.35$).

Site-Specific Tagged Mercury Deposition

Detroit (Livernois)

The CMAQ Model BASE CASE simulation mercury wet- and dry-deposition at the Detroit (Livernois) site for Calendar Year 2005, expressed in terms of tagged categories, is presented in Figure 12. Overall, the total mercury deposition to the site for Calendar Year 2005 was estimated to be 43.3 µg/m^2 (Wet: 17.7 µg/m^2, Dry: 25.6 µg/m^2). As can be seen, global sources were responsible for 54 percent of the total mercury wet-deposition, with Michigan-based incineration sources contributing about 12 percent and coal-fired EGUs contributing about nine percent to the total wet-deposition at the site. With respect to total mercury dry-deposition, global sources were responsible for approximately 35 percent of the total mercury dry-deposition, with Michigan-based incineration sources contributing about 20 percent and other Michigan-based sources (otherwise not tagged) accounting for about 16 percent of the total. The predominance of the incineration signature is not surprising given that there are two incineration sources within the Detroit metropolitan area.

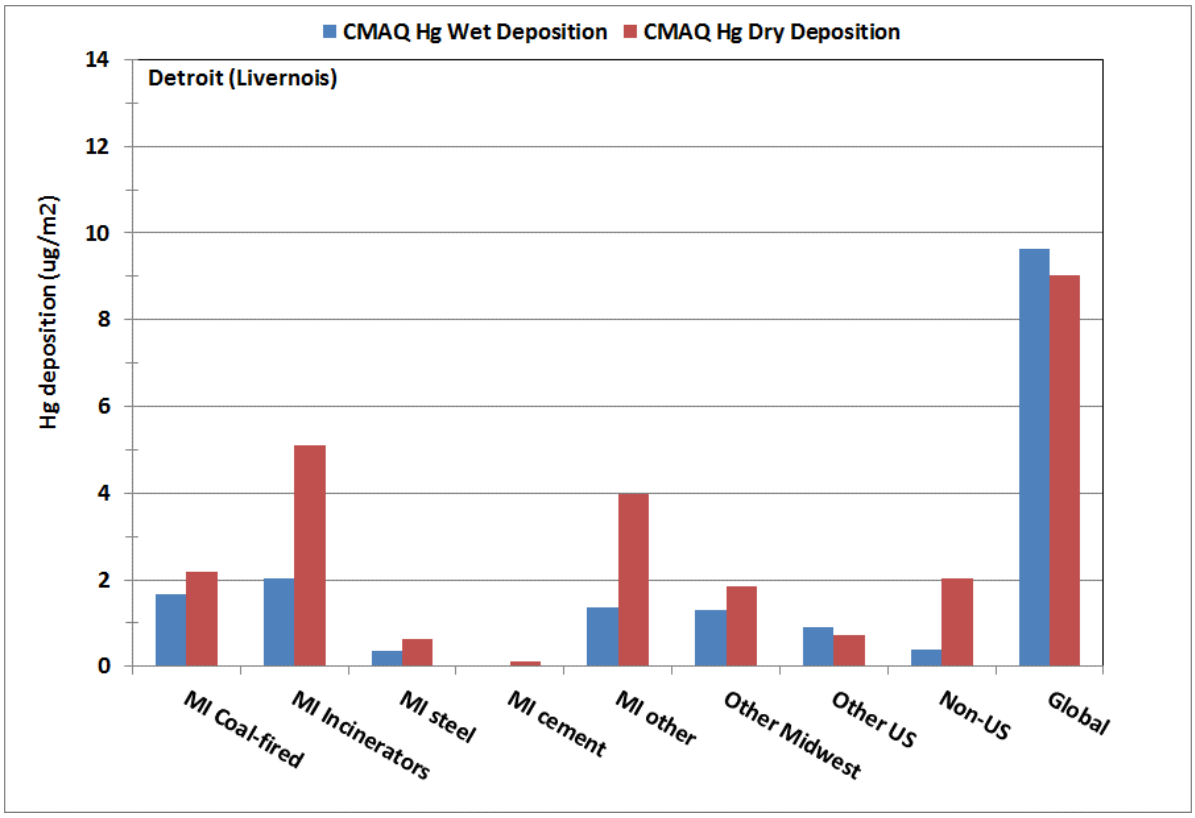

Figure 12. Calendar Year 2005 CMAQ Model BASE CASE simulation Mercury Wet- and Dry-deposition (µg/m^2) at Detroit (Livernois), MI for tagged emissions categories.

Dexter

The CMAQ Model BASE CASE simulation mercury wet- and dry-deposition at the Dexter, Michigan site for Calendar Year 2005, expressed in terms of tagged categories, is presented in Figure 13. Overall, the total mercury deposition to the site for Calendar Year 2005 was estimated to be 18.1 $\mu g/m^2$ (Wet: 10.1 $\mu g/m^2$, Dry: 8.0 $\mu g/m^2$). As can be seen, global sources were again the most significant contributor, responsible for 77 percent of the total mercury wet-deposition, with other Midwest-based sources (Wisconsin, Illinois, Indiana and Ohio) contributing about nine percent to the total mercury wet-deposition at the site. This result is consistent with some previous unpublished work by the PI, which focused on characterizing the type of meteorological events responsible for large mercury wet-deposition events. Those results suggested that long-term rainfall events, with an associated stationary front to the south of the Michigan state line, were often responsible for high mercury wet-deposition events across the northern Great Lakes, possibly due to the rainout of elevated mercury concentrations which flowed northward into Michigan from southern Great Lakes states.

With respect to total mercury dry-deposition, global sources were responsible for approximately 60 percent of the total mercury dry-deposition, with other Midwest-based sources contributing 14 percent and Michigan coal-fired EGUs contributing around nine percent.

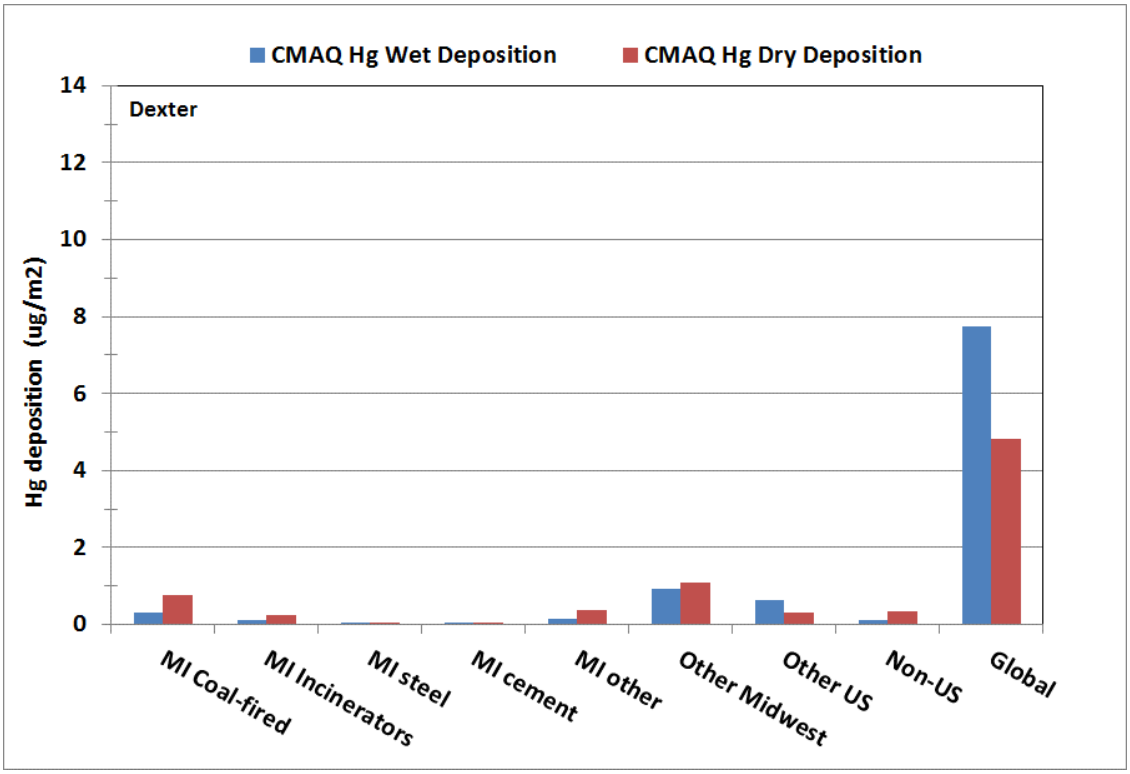

Figure 13. Calendar Year 2005 CMAQ Model BASE CASE Mercury Wet- and Dry-deposition ($\mu g/m^2$) at Dexter, MI field for tagged emissions categories.

Grand Rapids

The CMAQ Model BASE CASE simulation mercury wet- and dry-deposition at the Grand Rapids site for Calendar Year 2005, expressed in terms of tagged categories, is presented in Figure 14. Overall, the total mercury deposition to the site for Calendar Year 2005 was estimated to be 19.9 µg/m^2 (Wet: 12.6 µg/m^2, Dry: 7.3 µg/m^2). The general nature of the contributions to total mercury wet- and dry-deposition at this site is quite similar to that seen at the Dexter site. Namely, global sources were responsible for 69 percent of the total mercury wet-deposition, with other Midwest-based sources (Wisconsin, Illinois, Indiana and Ohio) contributing about 14 percent to the total mercury wet-deposition at the site. Both Other US sources (non-Michigan or Midwest) and Michigan-based coal-fired EGUs contributed approximately six percent. With respect to total mercury dry-deposition, global sources were responsible for approximately 57 percent of the total mercury dry-deposition, with other significant contributors being Other Midwest sources (15 percent), Other Michigan sources (11 percent) and Michigan coal-fired EGUs (10 percent).

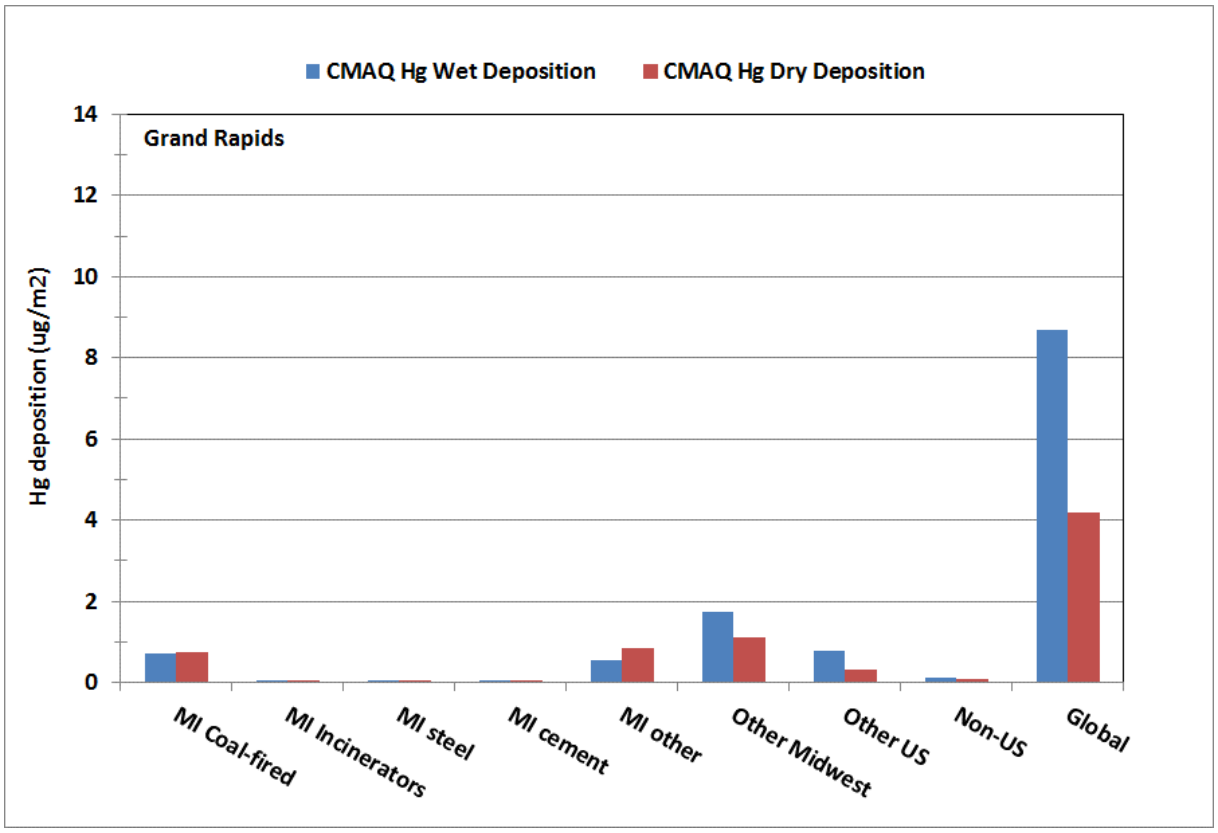

Figure 14. Calendar Year 2005 CMAQ Hg Wet- and Dry-deposition (µg/m^2) at Grand Rapids, MI for tagged emissions categories.

Flint

The CMAQ Model BASE CASE simulation mercury wet- and dry-deposition at the Flint site for Calendar Year 2005, expressed in terms of tagged categories, is presented in Figure 15. Overall, the total mercury deposition to the site for Calendar Year 2005 was estimated to be 42.2 µg/m^2 (Wet: 13.4 µg/m^2, Dry: 28.8 µg/m^2). As was found to be the case with the other sites presented thus far, the model predicts that a significant fraction of the deposition at the Flint site is the result global sources (65 percent of wet-deposition and 36 percent of the dry deposition). The reason that the global sources have a significantly lower percentage contribution to dry-deposition compared to wet-deposition is a result of our BASE CASE model prediction that the dominant contributor to dry-deposition at the site is from the municipal waste incineration sector (45 percent). The contribution of municipal waste incineration to the mercury wet-deposition flux at Flint is not insignificant, with the BASE CASE model predicting that 13 percent of wet-deposition flux at the site is likely from this sector.

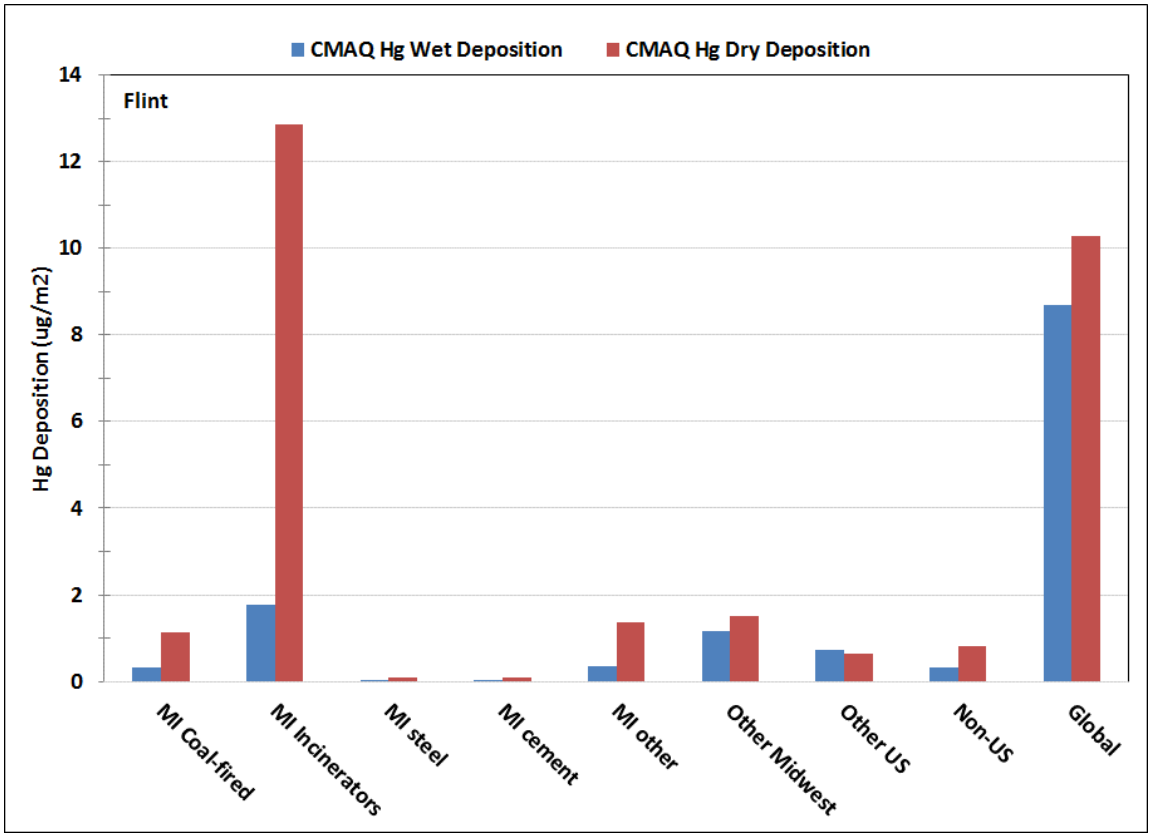

Figure 15. Calendar Year 2005 CMAQ Hg Wet- and Dry-deposition (µg/m^2) at Flint, MI for tagged emissions categories.

As one considers the total mercury deposition to the more northern sites, the predominance of the global source contribution increases. For the Pellston site (Figure 16), our CMAQ Model BASE

CASE simulation suggests that global sources account for 83 percent of the total mercury wet-deposition and 84 percent of the total dry-deposition. While the overall totals of deposition from other tag categories pale in comparison to the global source tag, the "Other Midwest" source tag contributes toward 7 percent of the wet-deposition to the site and 4 percent to the dry-deposition. The "Other US" source tag contributes six percent to the wet-deposition and three percent toward the dry-deposition to the site. Overall, the total mercury deposition to the site for Calendar Year 2005 was estimated to be 13.5 µg/m^2 (Wet: 11.1 µg/m^2, Dry: 2.4 µg/m^2). The CMAQ Model BASE CASE results for the Eagle Harbor site (Figure 17) are quite similar to those predicted for the Pellston site, with the global sources being far and away the most significant contributor to the total mercury deposition at the site, accounting for 89 percent of the total mercury wet-deposition and 93 percent of the total mercury dry-deposition to the site. Overall, the total mercury deposition to the site for Calendar Year 2005 was estimated to be 16.2 µg/m^2 (Wet: 11.6 µg/m^2, Dry: 4.6 µg/m^2).

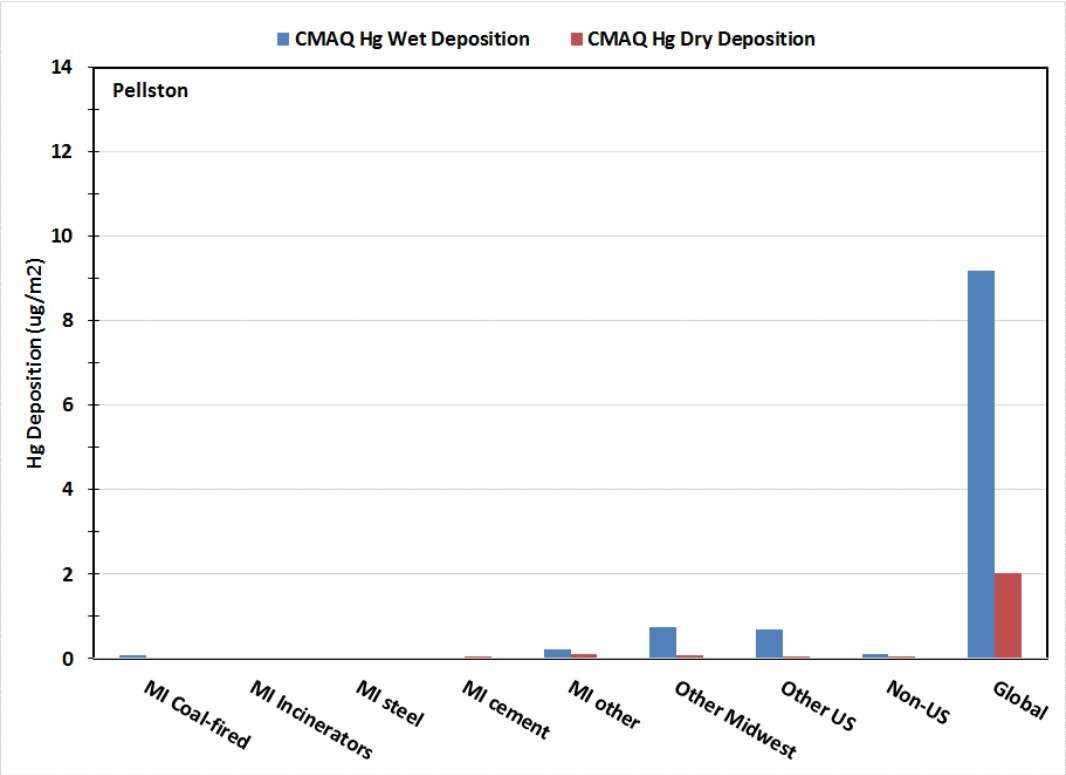

Figure 16. Calendar Year 2005 CMAQ Model BASE CASE simulation Mercury Wet- and Dry-deposition (µg/m^2) at Pellston, MI for tagged emissions categories.

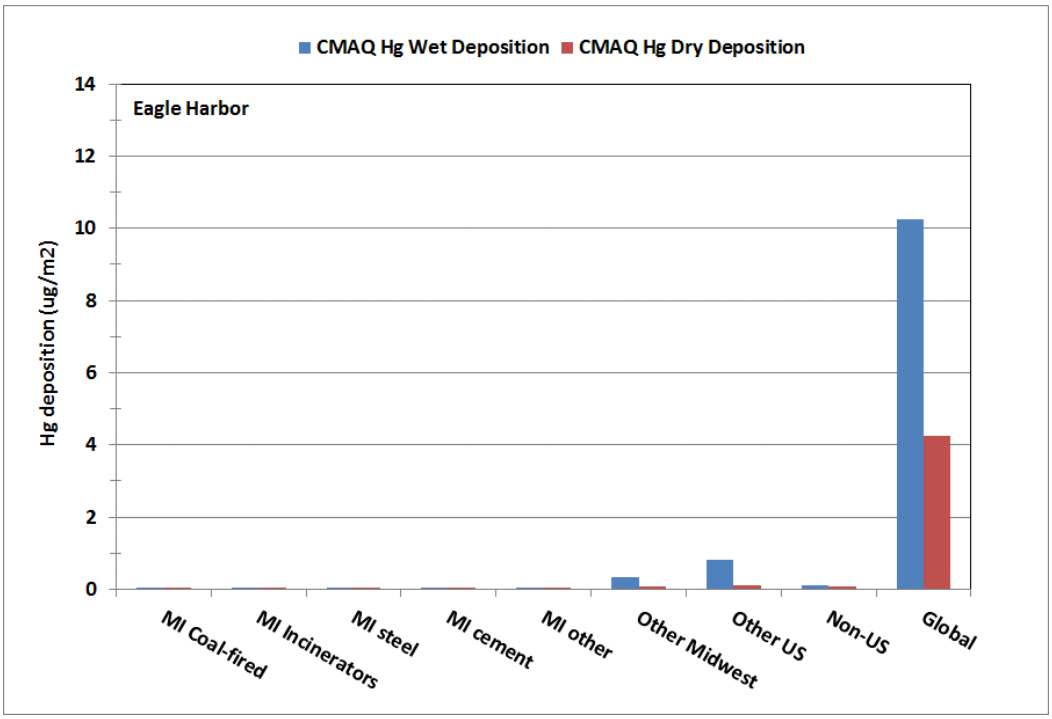

Figure 17. Calendar Year 2005 CMAQ Model BASE CASE Mercury Wet- and Dry-deposition ($\mu g/m^2$) at Eagle Harbor, MI for tagged emissions categories.

CMAQ Model REDUCED EMISSIONS SCENARIO Estimates

One of the primary objectives of this work was to provide an estimate of the total mercury deposition across the State of Michigan, including determining the relative contribution of various source categories/regions to that deposition through the use of emissions "tagging'. Of additional importance was the determination of the magnitude of potential reductions in total mercury deposition (wet- and dry-) to locations within the State of Michigan, which might come from reductions in mercury emissions within the State of Michigan.

At the request of the MDEQ, we estimated the total mercury deposition to a number of sites within the State of Michigan that could come from a 90 percent reduction in total mercury emissions from Michigan coal-fired EGUs, and an 82 percent reduction in total mercury emissions from all other sources within the State of Michigan. To obtain the total mercury deposition estimates from this CMAQ Model REDUCED EMISSIONS SCENARIO, we estimated the total deposition after reductions using the following relation:

Total Mercury Wet-Deposition = 0.10*Total Mercury Wet-Deposition (MEIC tag) + 0.18* Total Mercury Wet-Deposition (All other MI tags) + Remaining Total Mercury Wet-Deposition (BASE CASE)

Total Mercury Dry-Deposition = 0.10*Total Mercury Dry-Deposition (MEIC tag) + 0.18* Total Mercury Dry-Deposition (All other MI tags) + Remaining Total Mercury Dry-Deposition (BASE CASE)

We felt that this approach was justified given the linearity between total mercury emissions and total mercury deposition demonstrated earlier in this document. Based upon this approach, the results of the CMAQ Model REDUCED EMISSIONS SCENARIO are presented in Appendix D.

In summary, the greatest impact from the calculated emission reductions were generally seen in the estimates of the total mercury dry-deposition to the sites. This would seem reasonable, given that it is typically assumed that dry-deposition is dominated by GOM and PBM, both of which typically deposit near their sources. On a total magnitude and percentage basis, the greatest estimated reductions were found at our Detroit (Livernois) and Flint sites. For the Detroit (Livernois) location, it was estimated that the total mercury wet-deposition would decrease from 17.7 to 13.1 µg/m2 (26 percent reduction), while the total mercury dry-deposition would decrease from 25.6 µg/m2 to 15.6 µg/m2 (39 percent reduction). For the Flint location, it was estimated that the total mercury wet-deposition would decrease from 13.4 to 11.3 µg/m2 (16 percent reduction), while the total mercury dry-deposition would decrease from 28.8 µg/m2 to 16.0 µg/m2 (45 percent reduction).

The Grand Rapids and Dexter locations were predicted to experience significant total mercury deposition reductions, but primarily with respect to total mercury dry-deposition. Grand Rapids was predicted to obtain a nine percent reduction in total mercury wet-deposition and a 19 percent reduction in total mercury dry-deposition. Dexter was predicted to obtain a six percent reduction in total mercury wet-deposition and a 16 percent reduction in total mercury dry-deposition. Reductions for total mercury wet- and dry-deposition for the Pellston site was predicted to be three and six percent, respectively. Reductions for total mercury wet- and dry-deposition for the Eagle Harbor site were predicted to be less than one percent for both categories.

CMAQ Model REDUCED EMISSIONS SCENARIO Estimates (Statewide Totals)

As part of the Statewide Michigan Mercury TMDL (LimnoTech, 2013), the REMSAD modeling effort resulted in a prediction of a statewide mercury deposition of 18.6 µg/m2. The BASE CASE CMAQ Regional Chemical Modeling results from this study resulted in an estimated statewide mercury deposition of 21.0 µg/m2 (Wet-deposition: 12.6 µg/m2; Dry-Deposition: 8.4 µg/m2). Using our tagged species output, we calculated the statewide, total mercury deposition from three reduced emission scenarios: (1) 90% reduction in mercury emissions from coal-fired EGU sources within Michigan, (2) 82% reduction in mercury emissions from all Michigan anthropogenic sources (including wildfire emissions) and (3) 90% reduction in mercury emissions from coal-fired EGU sources within Michigan and 82% reduction in mercury emissions from all

Michigan anthropogenic sources (including wildfire emissions). The results of these calculations are presented in Table 13.

For the scenario characterized by a 90% reduction in coal-fired EGUs within the state of Michigan, the resulting estimated deposition was 20.3 µg/m2 (Wet-deposition: 12.2 µg/m2; Dry-Deposition: 8.1 µg/m2). For the scenario characterized by an 82% reduction in all Michigan anthropogenic sources, the resulting estimated deposition was 19.5 µg/m2 (Wet-deposition: 12.0 µg/m2; Dry-Deposition: 7.5 µg/m2). For the scenario characterized by a 90% reduction in mercury emissions from coal-fired EGU sources within Michigan and 82% reduction in mercury emissions from all Michigan anthropogenic sources, the resulting estimated deposition was 19.4 µg/m2 (Wet-deposition: 12.0 µg/m2; Dry-Deposition: 7.5 µg/m2).

Table 133. Modeled emissions from Michigan and surrounding states from CMAQ Model BASE CASE simulation.

		Mercury Emissions Reduction Scenario		
	CMAQ BASE CASE	90% Reduction in Michigan EGU Emissions	82% Reduction in all Michigan Anthropogenic Emissions	Combined 90% Reduction in EGU and 82% Reduction in All Other Michigan Antrhopogenic emissions
Wet-deposition (ug/m2)	12.6	12.2	12.0	12.0
Dry-deposition (ug/m2)	8.4	8.1	7.5	7.5
Total Deposition (ug/m2)	21.0	20.3	19.5	19.4

Overall, each of the three emissions reduction scenario calculations resulted in less than a 10% reduction in the statewide deposition of total mercury. These results are consistent with previous discussions of the predominant role played by emissions outside of the state of Michigan (both regional and global).

IV. Conclusions

Hourly, three dimensional meteorological fields were modeled for Calendar Year 2005 using the Weather Research and Forecasting (WRF) model. The meteorological fields were then used in concert with the U.S. Environmental Protection Agency's (USEPA) 2005 National Emissions Inventory (and updated emissions provided for the State of Michigan by the MDEQ) as input into the Sparse Matrix Operator Kernel Emissions (SMOKE) Modeling System to generate hourly emissions of mercury and other important chemical species. In turn, these emissions (and the WRF model output) were used as input into the USEPA's Community Multi-scale Air Quality Model (CMAQ) to generate hourly ambient speciated mercury concentrations and atmospheric deposition (both wet- and dry-) over the project's three modeling domains (36km, 12km and 4km). The latter domain (4km) focused upon the State of Michigan. Through the use of an emissions "tagging" approach implemented for this study, an additional goal was to estimate the relative contribution of various source types within the State of Michigan (coal-fired electric generation units, municipal waste incarnation, metallurgical processing, cement production and

all other sources in Michigan), as well as the contribution from surrounding states, the remainder of the continental United States and global sources.

For the purpose of this report, a series of locations from around the State of Michigan were chosen for use in presenting and evaluating the CMAQ regional chemical model results for our CMAQ Model BASE CASE simulation. These sites were Detroit, Dexter, Grand Rapids, Flint, Pellston and Eagle Harbor. These sites were primarily chosen given that the project investigators possessed ambient speciated mercury concentrations data from two of the sites (Detroit and Dexter), as well as mercury wet-deposition data from the other sites Calendar Year 2005. This data was used for the evaluation of the model performance for wet-deposition at these sites. A complete year of wet-deposition data was not available for the Flint site and thus it was not included in the comparison between modeled and measured wet-deposition.

Overall, the largest total mercury deposition was predicated for the Detroit (Livernois) site, with 43.3 $\mu g/m^2$ (Wet: 17.7 $\mu g/m^2$, Dry: 25.6 $\mu g/m^2$), with Flint having the second highest total at 42.2 $\mu g/m^2$ (Wet: 13.4 $\mu g/m^2$, Dry: 28.8 $\mu g/m^2$). Total mercury deposition was predicted to decrease significantly for the locations that were more distant from local anthropogenic sources and thus relatively less impacted by such sites: Grand Rapids 19.9 $\mu g/m^2$ (Wet: 12.6 $\mu g/m^2$, Dry: 7.3 $\mu g/m^2$), Dexter 18.1 $\mu g/m^2$ (Wet: 10.1 $\mu g/m^2$, Dry: 8.0 $\mu g/m^2$), Eagle Harbor 16.2 $\mu g/m^2$ (Wet: 11.6 $\mu g/m^2$, Dry: 4.6 $\mu g/m^2$), and Pellston 13.5 $\mu g/m^2$ (Wet: 11.1 $\mu g/m^2$, Dry: 2.4 $\mu g/m^2$).

The results suggest that, in general, global sources of mercury represent the largest contributor to both wet- and dry-deposition for the selected locations within the State of Michigan that were highlighted in this report. Only at the two most urban sites that were highlighted (Detroit (Livernios) and Flint) did sources within the State of Michigan make a substantial contribution. In Detroit, sources from within the State of Michigan contributed 32 percent to the total mercury wet-deposition and 47 percent to the total mercury dry-deposition. In Flint, sources from within the State of Michigan contributed 19 percent to the total mercury wet-deposition and 54 percent to the total mercury dry-deposition. In Detroit, the largest contributions from tagged sources were waste incineration and coal-fired electric generation units. In Flint, waste incineration was by far the largest in-state contributor to the total mercury deposition there.

Finally, estimates were made as to the potential impact of a mercury emissions reduction strategy of reducing in-state coal-fired electric generating units by 90 percent and all other in-state mercury emissions by 82 percent. Not surprisingly, the two sites that saw the most significant reduction in estimated total deposition were Detroit (Livernois) and Flint. The remaining sites, for which global sources were estimated to provide the dominant contribution, saw a limited reduction in total mercury deposition.

V. Acknowledgements

This research project is dedicated to the memory of Dr. Gerald Keeler, the founding Director of the University of Michigan Air Quality Laboratory, who passed away during the performance of this work. We would like to thank Mr. Dennis McGeen (MDEQ) for his assistance in the preparation of the raw emissions databases used in this project. We would also like to thank Ed Pniak (USEPA), Christine Urban (USEPA) and Joy Taylor-Morgan (MDEQ) for their patience and guidance. We would like to thank the Information Technology staff at the University of Michigan for their assistance over the course of this project. This work was funded through the USEPA's Great Lakes Restoration Initiative (Grant Number GL-00605).

Appendix A: Raw Emissions Files Used As Input into SMOKE Processing Program

Area Source Files (United States)

arinv_nonpt_cap_2005_TCEQ_Oklahoma_OilGas_28may2010_v0_orl.txt
arinv_nonpt_pf4_cap_nopfc_28may2010_v3_orl.txt
arinv_nonpt_pf4_hap_nopfc_nobafmpesticidesplus_28may2010_v1_rev083012_orl.txt
arinv_pfc_2002_caphap_27dec2007_v0_orl.txt
arinv_nonpt_cap_2005_WRAP_OilGas_04feb2009_v0_orl.txt
arinv_afdust_2002ad_xportfrac_26sep2007_v0_orl.txt
arinv_ag_cap2002nei_06nov2006_v0_orl.txt
arinv_avefire_2002ce_21dec2007_v1_withhg_ida.txt

Area Source Files (Canada and Mexico)

arinv_canada_afdust_xportfrac_cap_2006_03feb2009_v0_orl.txt
arinv_canada_oarea_cap_2006_02mar2009_v3_orl.txt
arinv_canada_ag_cap_2006_03feb2009_v0_orl.txt
arinv_nonpt_mexico_border1999_21dec2006_v0_ida.txt
arinv_nonpt_mexico_interior1999_21dec2006_v0_ida.txt
arinv_nonpt_hg_mexico_all1999_fltmdl_21may2010_v4_ida.txt
arinv_area_canada_hg_2000_noduplicates_23jul2008_v0_ida.txt

Mobile Source Files (Onroad, United States)

mbinv_onroad_calif_caphap_2005v2_revised_<mon>_29jun2010_v0_orl.txt
mbinv_on_noadj_nmim_not2moves_2005cr_<mon>_04MAY2010_04may2010_v0_orl.txt
mbinv_on_noadj_MOVES_2005cr_<mon>_06MAY2010_06may2010_v0_orl.txt
on_moves_startpm/mbinv_on_moves_startpm_2005cr_<mon>_06MAY2010_06may2010_v0_orl.txt
on_moves_runpm/mbinv_on_moves_runpm_2005cr_<mon>_06MAY2010_06may2010_v0_orl.txt

Mobile Source Files (Onroad, Canada and Mexico)

mbinv_canada_onroad_cap_2006_04feb2009_v0_062911_orl.txt
mbinv_onroad_mexico_border1999_21dec2006_v0_ida.txt
mbinv_onroad_mexico_interior1999_21dec2006_v0_ida.txt

Mobile Source Files (Nonroad, United States)

arinv_nonroad_caps_2005v2_<mon>_revised_08sep2008_v0_orl.txt
arinv_nonroad_calif_caphap_2005v2_revised_<mon>_23jun2010_v0_orl.txt
arinv_nonroad_haps_2005v2_<mon>A_revised_05sep2008_v0_orl.txt
arinv_nonroad_haps_2005v2_<mon>B_revised_05sep2008_v0_orl.txt
alm_no_c3/arinv_lm_no_c3_hap2002v4_20feb2009_v0_orl.txt
alm_no_c3/arinv_lm_no_c3_cap2002v3_20feb2009_v0_orl.txt

Mobile Source Files (Nonroad, Canada and Mexico)

arinv_canada_aircraft_cap_2006_04feb2009_v0_rev_orl.txt
arinv_canada_marine_cap_2006_03feb2009_v0_rev_orl.txt
arinv_canada_offroad_cap_2006_04feb2009_v0_rev_orl.txt
arinv_canada_rail_cap_2006_03feb2009_v0_rev_orl.txt
arinv_nonroad_mexico_border1999_21dec2006_v0_ida.txt
arinv_nonroad_mexico_interior1999_21dec2006_v0_ida.txt

Point Source Files (United States)

ptinv_ptipm_cap2005v2_revised12mar2009_15jul2010_v5_orl.txt
ptinv_ptipm_hap2005v2_allHAPs_revised12mar2009_14jul2010_v1_rev080812_nohg_orl.txt
ptinv_ptnonipm_hap2005v2_revised_08jul2010_v2_rev080812_nohg_orl.txt
ptinv_2005_ICR_BoilerMACT_Hg_ptnonipm_20aug2010_v0_rev080212_orl.txt
ptinv_2005_ptnonipm_natahg_minus_boilermacticr_17aug2010_v0_rev082412_orl.txt

ptinv_2005_ptipm_natahg_minus_boilermacticr_17aug2010_v0_rev073112_orl.txt
ptinv_ptnonipm_xportfrac_cap2005v2_20nov2008_revised_22jul2010_v5_orl.txt
ptinv_ptnonipm_hap2005v2_revised_08jul2010_v2_orl.txt
ptinv_ptnonipm_caphap_ethanol_plant_additions_2005_30jun2010_v3_orl.txt
ptinv_ptnonipm_xportfrac_2005cap_v1_from_2005ai_ND_ADM_plant_30jun2010_v0_orl.txt
ptinv_ptnonipm_2005hap_v1_from_2005ai_ND_ADM_plant_30jun2010_v0_orl.txt
ptinv_ptnonipm_offshore_oil_cap2005v2_20nov2008_20nov2008_v0_orl.txt
ptinv_eca_imo_FINAL_c3_baf_vochaps_2005_us_24jun2010_24jun2010_v0_orl.txt
ptinv_eca_imo_FINAL_c3_caps_2005_us_24jun2010_24jun2010_v0_orl.txt

Point Source Files (Canada and Mexico)

ptinv_point_canada_hg_2000_08sep2008_v1_ida.txt
ptinv_canada_point_2006_orl_09mar2009_v2_orl.txt
ptinv_canada_point_cb5_2006_orl_10mar2009_v0_orl.txt
ptinv_canada_point_uog_2006_orl_02mar2009_v0_orl.txt
ptinv_mexico_border99_03mar2008_v1_ida.txt
ptinv_mexico_interior99_05feb2007_v0_ida.txt
ptinv_eca_imo_FINAL_c3_baf_vochaps_2005_canada_24jun2010_28jun2010_v0_orl.txt
ptinv_eca_imo_FINAL_c3_caps_2005_canada_24jun2010_28jun2010_v0_orl.txt

Files that were created/updated for this modeling effort.
Redundant file that was erroneously left in emissions list and resulted in over estimate of mercury emissions.

Appendix B: Emissions correction factors and Emissions Summary

Table B1: Emissions Ratios for State of Michigan Tags

Tag Name	Total Hg With (tons per day)	Total Hg Without (tons per day)	Total Hg Ratio Without/With
MIEC	4.13E-03	3.96E-03	0.96
MIMET	4.05E-04	4.05E-04	1.00
MICM	1.63E-03	8.60E-04	0.53
MIIN	4.89E-04	4.19E-04	0.86
MI OTHER	5.65E-03	3.47E-03	0.61
Total Hg	1.23E-02	9.12E-03	
Total Hg (pounds per year)	8,984	6,656	

Table B2: Emissions Ratios for Surrounding States Tags

State	Total Hg Ratio Without/With
Illinois	0.76
Indiana	0.72
Ohio	0.44
Wisconsin	0.75

Table B3: Emissions Ratios for Other US States and Territories

Region	Total Hg Ratio Without/With
Other US States and Territories	0.74

Table B4. Corrected Emissions for Michigan Counties by Emissions Category

FIPS	County	Point (tpy)	Area (tpy)	Onroad Mobile (tpy)	Nonroad Mobile (tpy)	Total (tpy)
26001	Alcona Co	2.48E-05	6.83E-04	1.98E-04	2.65E-05	9.32E-04
26003	Alger Co	7.70E-04	3.84E-04	4.18E-06	2.09E-06	1.16E-03
26005	Allegan Co	1.43E-04	1.00E-03	8.20E-06	2.33E-06	1.16E-03
26007	Alpena Co	2.66E-01	2.22E-03	3.67E-05	5.27E-06	2.69E-01
26009	Antrim Co	3.49E-05	1.66E-02	2.39E-04	2.27E-05	1.69E-02
26011	Arenac Co	4.11E-05	1.23E-03	1.43E-05	2.03E-06	1.29E-03
26013	Baraga Co	1.99E-05	2.96E-03	9.52E-05	3.53E-06	3.08E-03
26015	Barry Co	5.23E-05	1.15E-02	1.83E-04	1.53E-05	1.18E-02
26017	Bay Co	1.27E-01	1.22E-03	3.66E-05	4.64E-06	1.29E-01
26019	Benzie Co	2.57E-05	1.36E-02	2.68E-04	9.83E-06	1.39E-02
26021	Berrien Co	7.27E-03	2.30E-03	3.68E-05	1.30E-05	9.62E-03
26023	Branch Co	2.60E-04	6.65E-03	1.07E-04	5.75E-06	7.02E-03
26025	Calhoun Co	1.30E-03	3.88E-02	7.04E-04	3.67E-05	4.08E-02
26027	Cass Co	7.45E-02	1.28E-03	2.47E-05	4.89E-06	7.58E-02
26029	Charlevoix Co	5.99E-02	1.06E-02	2.58E-04	1.35E-05	7.08E-02
26031	Cheboygan Co	2.99E-03	1.57E-03	1.72E-05	2.37E-06	4.58E-03
26033	Chippewa Co	1.32E-03	1.41E-03	2.53E-05	1.64E-06	2.75E-03
26035	Clare Co	4.13E-05	1.69E-03	3.41E-05	3.39E-06	1.77E-03
26037	Clinton Co	1.29E-04	1.32E-03	3.50E-05	9.77E-06	1.50E-03
26039	Crawford Co	4.52E-05	3.57E-03	4.66E-05	4.34E-06	3.67E-03
26041	Delta Co	1.03E-02	5.61E-03	9.18E-05	1.23E-05	1.61E-02
26043	Dickinson Co	2.28E-02	4.52E-03	1.41E-04	4.90E-06	2.74E-02
26045	Eaton Co	2.85E-02	1.89E-03	2.71E-05	5.45E-06	3.04E-02
26047	Emmet Co	1.02E-04	2.03E-03	3.26E-05	6.17E-06	2.17E-03
26049	Genesee Co	1.21E-02	1.98E-03	2.45E-05	2.37E-06	1.41E-02
26051	Gladwin Co	3.61E-05	9.91E-04	1.25E-05	1.51E-06	1.04E-03
26053	Gogebic Co	1.97E-04	1.18E-02	2.37E-04	1.27E-05	1.23E-02
26055	Grand Traverse Co	2.21E-03	1.07E-02	2.08E-04	1.10E-05	1.31E-02
26057	Gratiot Co	1.28E-05	5.22E-03	1.22E-04	5.95E-06	5.36E-03
26059	Hillsdale Co	3.35E-02	3.45E-03	5.57E-05	4.61E-06	3.70E-02
26061	Houghton Co	6.29E-05	4.29E-03	7.16E-05	4.87E-06	4.43E-03
26063	Huron Co	2.65E-02	2.22E-03	3.57E-05	7.55E-06	2.88E-02
26065	Ingham Co	7.54E-02	7.08E-03	1.59E-04	1.02E-05	8.26E-02
26067	Ionia Co	6.83E-04	6.13E-03	1.07E-04	6.85E-06	6.93E-03
26069	Iosco Co	3.34E-05	1.25E-03	2.09E-05	4.95E-06	1.31E-03
26071	Iron Co	6.70E-05	1.24E-03	1.52E-05	1.59E-06	1.32E-03
26073	Isabella Co	7.55E-04	1.17E-03	1.54E-05	1.36E-06	1.94E-03
26075	Jackson Co	1.41E-02	2.40E-03	3.73E-05	8.82E-06	1.65E-02
26077	Kalamazoo Co	9.47E-03	2.77E-03	6.60E-05	2.51E-06	1.23E-02
26079	Kalkaska Co	3.09E-05	1.99E-03	4.60E-05	6.32E-06	2.07E-03
26081	Kent Co	1.74E-02	2.25E-03	2.61E-05	1.84E-06	1.97E-02
26083	Keweenaw Co	1.08E-06	2.36E-03	4.36E-05	2.73E-06	2.41E-03
26085	Lake Co	2.36E-05	4.78E-03	6.92E-05	5.34E-06	4.88E-03
26087	Lapeer Co	5.65E-05	1.01E-03	9.83E-06	1.60E-06	1.08E-03
26089	Leelanau Co	1.55E-05	3.88E-03	6.50E-05	6.39E-06	3.96E-03
26091	Lenawee Co	3.46E-02	9.10E-03	2.06E-04	6.20E-06	4.39E-02
26093	Livingston Co	1.19E-04	1.89E-03	2.65E-05	5.60E-06	2.05E-03
26095	Luce Co	4.19E-05	2.02E-03	2.98E-05	5.88E-06	2.09E-03

Table B4. Continued

FIPS	County	Point (tpy)	Area (tpy)	Onroad Mobile (tpy)	Nonroad Mobile (tpy)	Total (tpy)
26097	Mackinac Co	2.29E-05	1.12E-02	4.54E-05	7.33E-06	1.12E-02
26099	Macomb Co	1.58E-02	7.00E-03	1.40E-04	5.25E-06	2.30E-02
26101	Manistee Co	2.25E-02	1.28E-03	3.45E-05	2.08E-06	2.38E-02
26103	Marquette Co	9.51E-02	4.00E-03	5.33E-05	5.95E-06	9.92E-02
26105	Mason Co	8.37E-03	2.93E-03	2.69E-05	4.14E-06	1.13E-02
26107	Mecosta Co	6.42E-05	1.00E-02	2.45E-04	1.74E-05	1.03E-02
26109	Menominee Co	4.76E-03	4.22E-03	8.75E-05	3.20E-06	9.07E-03
26111	Midland Co	8.01E-05	5.61E-03	9.98E-05	3.86E-06	5.80E-03
26113	Missaukee Co	1.23E-05	2.22E-02	4.40E-04	2.12E-05	2.27E-02
26115	Monroe Co	4.79E-01	1.13E-03	1.95E-05	3.21E-06	4.81E-01
26117	Montcalm Co	1.21E-04	5.37E-02	7.80E-04	4.96E-05	5.47E-02
26119	Montmorency Co	3.71E-03	1.97E-03	3.23E-05	5.84E-06	5.72E-03
26121	Muskegon Co	1.11E-01	1.17E-03	1.28E-05	2.61E-06	1.13E-01
26123	Newaygo Co	3.52E-05	1.90E-03	3.49E-05	2.81E-06	1.97E-03
26125	Oakland Co	5.38E-03	1.81E-02	3.10E-04	1.10E-05	2.38E-02
26127	Oceana Co	1.05E-02	1.82E-03	2.08E-05	2.41E-06	1.24E-02
26129	Ogemaw Co	4.46E-05	7.87E-02	1.56E-03	7.51E-05	8.04E-02
26131	Ontonagon Co	1.99E-02	3.08E-03	4.93E-05	8.84E-06	2.30E-02
26133	Osceola Co	1.14E-04	5.35E-03	7.41E-05	6.15E-06	5.54E-03
26135	Oscoda Co	8.08E-06	1.29E-01	2.22E-03	9.00E-05	1.32E-01
26137	Otsego Co	2.09E-05	4.77E-03	1.84E-05	4.21E-06	4.82E-03
26139	Ottawa Co	2.15E-01	1.76E-03	3.55E-05	6.58E-06	2.16E-01
26141	Presque Isle Co	3.85E-05	1.73E-03	4.04E-05	2.12E-06	1.81E-03
26143	Roscommon Co	8.72E-05	2.20E-03	2.96E-05	2.72E-06	2.32E-03
26145	Saginaw Co	4.94E-02	3.05E-03	5.52E-05	3.61E-06	5.25E-02
26147	St Clair Co	2.77E-01	7.48E-03	1.52E-04	1.05E-05	2.85E-01
26149	St Joseph Co	8.90E-03	3.09E-03	4.94E-05	3.63E-06	1.20E-02
26151	Sanilac Co	2.52E-03	4.35E-03	7.07E-05	6.93E-06	6.95E-03
26153	Schoolcraft Co	2.60E-02	2.31E-03	4.70E-05	3.35E-06	2.84E-02
26155	Shiawassee Co	6.37E-04	1.52E-03	3.06E-05	1.19E-05	2.20E-03
26157	Tuscola Co	1.32E-02	2.88E-02	5.66E-04	1.82E-05	4.25E-02
26159	Van Buren Co	8.77E-05	2.88E-03	4.95E-05	3.32E-06	3.02E-03
26161	Washtenaw Co	1.80E-03	1.56E-02	3.06E-04	1.36E-05	1.78E-02
26163	Wayne Co	4.10E-01	1.17E-03	1.43E-05	3.19E-06	4.11E-01
26165	Wexford Co	2.65E-02	3.41E-03	4.25E-05	1.00E-05	3.00E-02
Total Mercury Emissions (tpy)		**2.64**	**0.68**	**1.22E-02**	**7.79E-04**	**3.33**
2005 Michigan DEQ Mercury Inventory (tpy)		**2.57**	**0.67**	**1.73E-04**	**2.57E-03**	**3.24**

Appendix C: CMAQ Model-Measurement Comparison for Ambient Concentrations at Detroit and Dexter

Detroit (Fort Street/Livernois) Sites															
	CMAQ	CMAQ	CMAQ		UMAQL	UMAQL	UMAQL		Mean Absolute Error				Mean Error		
	GEM	GOM	PHG		GEM	GOM	PHG		GEM	GOM	PHG		GEM	GOM	PHG
	ng/m3	pg/m3	pg/m3		ng/m3	pg/m3	pg/m3		ng/m3	pg/m3	pg/m3		ng/m3	pg/m3	pg/m3
January															
Average	1.4	25	45		1.8	5	9		0.5	21	37		-0.4	20	36
Std Dev	0.2	23	31		0.5	4	5								
0.10	1.2	9	16		1.3	2	4								
0.90	1.6	50	72		2.4	10	15								
Correlation [r]	0.44	-0.12	0.07												
February															
Average	1.3	27	62		2.3	6	14		1.0	26	50		-1.0	26	48
Std Dev	0.3	25	45		0.7	4	11								
0.10	1.0	7	16		1.6	1	3								
0.90	1.6	50	100		3.0	12	28								
Correlation [r]	0.58	0.37	0.35												
March															
Average	1.2	26	77		1.4	2	7		0.4	22	68		-0.2	23	71
Std Dev	0.2	18	37		0.4	2	4								
0.10	1.0	8	33		0.9	1	1								
0.90	1.3	44	123		1.8	4	12								
Correlation [r]	-0.20	-0.06	0.38												
April															
Average	1.1	29	60		2.1	15	8		1.0	8	26		-1.0	2	25
Std Dev	0.2	23	39		0.4	16	8								
0.10	1.1	3	11		1.6	5	0								
0.90	1.3	59	116		2.5	37	17								
Correlation [r]	0.02	0.74	0.38												
May															
Average	1.1	27	40		2.2	22	13		1.1	16	29		-1.1	5	27
Std Dev	0.2	27	32		0.6	19	12								
0.10	1.1	3	5		1.8	5	6								
0.90	1.3	76	84		2.8	50	19								
Correlation [r]	-0.01	0.59	0.41												
June															
Average	1.1	32	39		2.4	32	11		1.3	17	29		-1.3	-1	28
Std Dev	0.1	22	26		0.4	23	5								
0.10	1.0	4	7		1.9	8	3								
0.90	1.2	62	73		2.8	55	15								
Correlation [r]	-0.25	0.55	0.41												

Detroit (Fort Street/Livernois) Sites															
		CMAQ	CMAQ	CMAQ		UMAQL	UMAQL	UMAQL		Mean Absolute Error				Mean Error	
		GEM	GOM	PHG		GEM	GOM	PHG		GEM	GOM	PHG		GEM	GOM	PHG
		ng/m3	pg/m3	pg/m3		ng/m3	pg/m3	pg/m3		ng/m3	pg/m3	pg/m3		ng/m3	pg/m3	pg/m3
July																
Average		1.2	30	39		2.0	13	8		0.9	20	31		-0.9	17	31
Std Dev		0.1	21	25		0.7	14	7								
0.10		1.0	9	11		1.3	1	1								
0.90		1.3	63	67		3.0	33	17								
Correlation [r]		-0.07	0.43	0.18												
August																
Average		1.2	27	32		2.3	9	11		1.1	21	26		-1.1	18	21
Std Dev		0.2	24	25		0.8	7	12								
0.10		1.0	3	6		1.6	2	3								
0.90		1.3	60	62		3.2	20	17								
Correlation [r]		0.01	0.37	0.05												
September																
Average		1.5	33	43		2.1	22	10		0.7	16	31		-0.6	10	31
Std Dev		0.2	25	30		0.7	18	7								
0.10		1.4	10	13		1.5	5	3								
0.90		1.6	66	90		2.8	46	19								
Correlation [r]		-0.15	0.53	0.47												
October																
Average		1.5	35	46		2.2	10	10		0.6	30	40		-0.6	26	36
Std Dev		0.2	56	66		0.5	10	8								
0.10		1.4	2	3		1.6	1	2								
0.90		1.8	157	175		2.7	23	22								
Correlation [r]		-0.05	0.61	0.29												
November																
Average		1.5	22	32		3.3	12	17		1.8	15	19		-1.8	10	16
Std Dev		0.2	21	23		1.0	15	13								
0.10		1.4	7	11		2.3	1	2								
0.90		1.6	39	60		4.5	29	32								
Correlation [r]		0.39	0.29	0.59												
December																
Average		1.5	22	42		2.3	4	11		0.7	16	31		-0.7	16	30
Std Dev		0.3	20	26		0.5	5	8								
0.10		1.3	7	15		1.7	1	3								
0.90		1.9	53	88		2.8	9	20								
Correlation [r]		0.07	0.36	0.41												

Dexter Site															
	CMAQ	CMAQ	CMAQ		UMAQL	UMAQL	UMAQL		Mean Absolute Error				Mean Error		
	GEM	GOM	PHG		GEM	GOM	PHG		GEM	GOM	PHG		GEM	GOM	PHG
	ng/m3	pg/m3	pg/m3		ng/m3	pg/m3	pg/m3		ng/m3	pg/m3	pg/m3		ng/m3	pg/m3	pg/m3
January															
Average	1.3	12	32		1.6	3	10		0.2	9	23		-0.2	9	22
Std Dev	0.2	7	19		0.2	2	6								
0.10	1.2	5	12		1.4	1	4								
0.90	1.5	23	61		1.8	5	20								
Correlation [r]	0.25	0.39	0.45												
February															
Average	1.2	13	47		1.6	5	10		0.4	9	39		-0.4	9	37
Std Dev	0.3	8	29		0.2	3	7								
0.10	0.9	2	4		1.4	2	4								
0.90	1.5	24	82		1.8	8	17								
Correlation [r]	-0.07	0.04	0.29												
March															
Average	1.2	20	76		1.6	3	13		0.4	19	64		-0.4	17	64
Std Dev	0.1	12	37		0.2	4	10								
0.10	1.0	7	24		1.5	1	0								
0.90	1.3	37	120		1.8	5	25								
Correlation [r]	0.09	-0.32	0.26												
April															
Average	1.1	17	52		1.6	7	7		0.5	13	45		-0.5	11	45
Std Dev	0.2	13	34		0.2	10	5								
0.10	1.1	3	10		1.4	0	2								
0.90	1.2	34	96		1.7	14	14								
Correlation [r]	-0.27	0.38	0.55												
May															
Average	1.1	11	27		1.5	4	7		0.4	8	22		-0.4	7	20
Std Dev	0.1	9	23		0.1	6	2								
0.10	1.0	2	2		1.3	0	4								
0.90	1.2	24	55		1.7	9	10								
Correlation [r]	0.18	0.38	0.22												
June															
Average	1.0	12	24		1.3	3	6		0.3	11	20		-0.2	10	20
Std Dev	0.1	9	21		0.1	4	3								
0.10	1.0	3	4		1.2	0	3								
0.90	1.1	28	52		1.4	8	9								
Correlation [r]	-0.14	-0.06	0.12												

Dexter Site															
		CMAQ	CMAQ	CMAQ		UMAQL	UMAQL	UMAQL		Mean Absolute Error				Mean Error	
		GEM	GOM	PHG		GEM	GOM	PHG		GEM	GOM	PHG		GEM	GOM	PHG
		ng/m3	pg/m3	pg/m3		ng/m3	pg/m3	pg/m3		ng/m3	pg/m3	pg/m3		ng/m3	pg/m3	pg/m3
July															
Average		1.1	17	27		2.3	15	27		1.2	13	18		-1.2	11	13
Std Dev		0.1	12	19		0.5	10	17							
0.10		1.0	4	8		1.5	0	0							
0.90		1.2	30	46		2.8	26	41							
Correlation [r]		0.43	0.51	0.60											
August															
Average		1.1	15	23		1.0	1	2		0.2	14	21		0.1	14	21
Std Dev		0.1	12	17		0.2	5	2							
0.10		1.0	2	4		0.9	0	0							
0.90		1.2	33	49		1.3	1	4							
Correlation [r]		-0.19	0.32	-0.13											
September															
Average		1.4	22	36		1.2	3	3		0.3	19	33		0.2	19	33
Std Dev		0.2	14	24		0.3	4	2							
0.10		1.3	10	9		0.8	0	1							
0.90		1.5	35	61		1.5	7	4							
Correlation [r]		-0.13	0.33	0.24											
October															
Average		1.5	14	26		1.6	2	4		0.4	13	23		-0.1	13	22
Std Dev		0.2	13	25		0.4	2	3							
0.10		1.4	3	4		0.9	0	1							
0.90		1.6	32	57		1.9	4	8							
Correlation [r]		-0.25	-0.19	0.09											
November															
Average		1.4	12	25		1.5	2	7		0.2	10	18		0.0	10	18
Std Dev		0.2	6	16		0.2	2	4							
0.10		1.4	5	10		1.3	0	3							
0.90		1.5	21	54		1.7	6	13							
Correlation [r]		0.05	0.27	0.39											
December															
Average		1.5	10	28		1.3	2	10		0.1	13	22		0.0	13	22
Std Dev		0.2	7	17		0.0	1	3							
0.10		1.2	2	5		1.3	1	6							
0.90		1.6	18	44		1.4	3	12							
Correlation [r]		-0.25	-0.28	0.69											

Appendix D: Data Table for Emissions Reduction Scenario

Detroit - Livernois	BASE CASE		EMISSIONS REDUCTION CASE	
	Wet Deposition (ug/m2)	Dry Deposition (ug/m2)	Wet Deposition (ug/m2)	Dry Deposition (ug/m2)
MI Coal-fired	1.7	2.2	0.2	0.2
MI Incinerators	2.0	5.1	0.4	0.9
MI steel	0.3	0.6	0.1	0.1
MI cement	<0.1	0.1	<0.1	<0.1
MI other	1.4	4.0	0.2	0.7
Other Midwest	1.3	1.8	1.3	1.8
Other US	0.9	0.7	0.9	0.7
Non-US	0.4	2.0	0.4	2.0
Global	9.6	9.0	9.6	9.0
Total Deposition (ug/m2)	17.7	25.6	13.1	15.6
Percent Reduction			26.1	39.1

Pellston	BASE CASE		EMISSIONS REDUCTION CASE	
	Wet Deposition (ug/m2)	Dry Deposition (ug/m2)	Wet Deposition (ug/m2)	Dry Deposition (ug/m2)
MI Coal-fired	0.1	<0.1	<0.1	<0.1
MI Incinerators	<0.1	<0.1	<0.1	<0.1
MI steel	<0.1	<0.1	<0.1	<0.1
MI cement	<0.1	<0.1	<0.1	<0.1
MI other	0.2	0.1	<0.1	<0.1
Other Midwest	0.7	0.1	0.7	0.1
Other US	0.7	0.1	0.7	0.1
Non-US	0.1	<0.1	0.1	<0.1
Global	9.2	2.0	9.2	2.0
Total Deposition (ug/m2)	11.1	2.4	10.8	2.2
Percent Reduction			2.5	5.9

Grand Rapids	BASE CASE		EMISSIONS REDUCTION CASE	
	Wet Deposition (ug/m2)	Dry Deposition (ug/m2)	Wet Deposition (ug/m2)	Dry Deposition (ug/m2)
MI Coal-fired	0.7	0.7	0.1	0.1
MI Incinerators	<0.1	<0.1	<0.1	<0.1
MI steel	<0.1	<0.1	<0.1	<0.1
MI cement	<0.1	<0.1	<0.1	<0.1
MI other	0.6	0.8	0.1	0.2
Other Midwest	1.7	1.1	1.7	1.1
Other US	0.8	0.3	0.8	0.3
Non-US	0.1	0.1	0.1	0.1
Global	8.7	4.2	8.7	4.2
Total Deposition (ug/m2)	12.6	7.3	11.5	5.9
Percent Reduction			8.9	19.0

Eagle Harbor	BASE CASE		EMISSIONS REDUCTION CASE	
	Wet Deposition (ug/m2)	Dry Deposition (ug/m2)	Wet Deposition (ug/m2)	Dry Deposition (ug/m2)
MI Coal-fired	<0.1	<0.1	<0.1	<0.1
MI Incinerators	<0.1	<0.1	<0.1	<0.1
MI steel	<0.1	<0.1	<0.1	<0.1
MI cement	<0.1	<0.1	<0.1	<0.1
MI other	<0.1	<0.1	<0.1	<0.1
Other Midwest	0.3	0.1	0.3	0.1
Other US	0.8	0.1	0.8	0.1
Non-US	0.1	0.1	0.1	0.1
Global	10.2	4.3	10.2	4.3
Total Deposition (ug/m2)	11.6	4.6	11.5	4.5
Percent Reduction			0.5	0.9

Dexter	BASE CASE		EMISSIONS REDUCTION CASE	
	Wet Deposition (ug/m2)	Dry Deposition (ug/m2)	Wet Deposition (ug/m2)	Dry Deposition (ug/m2)
MI Coal-fired	0.3	0.7	<0.1	<0.1
MI Incinerators	0.1	0.2	<0.1	<0.1
MI steel	<0.1	0.1	<0.1	<0.1
MI cement	<0.1	<0.1	<0.1	<0.1
MI other	0.2	0.4	<0.1	0.1
Other Midwest	0.9	1.1	0.9	1.1
Other US	0.6	0.3	0.6	0.3
Non-US	0.1	0.3	0.1	0.3
Global	7.8	4.8	7.8	4.8
Total Deposition (ug/m2)	10.1	8.0	9.5	6.8
Percent Reduction			5.5	15.7

Flint	BASE CASE		EMISSIONS REDUCTION CASE	
	Wet Deposition (ug/m2)	Dry Deposition (ug/m2)	Wet Deposition (ug/m2)	Dry Deposition (ug/m2)
MI Coal-fired	0.3	1.1	<0.1	0.1
MI Incinerators	1.8	12.9	0.3	2.3
MI steel	<0.1	0.1	<0.1	<0.1
MI cement	<0.1	0.1	<0.1	<0.1
MI other	0.4	1.4	0.1	0.2
Other Midwest	1.2	1.5	1.2	1.5
Other US	0.7	0.7	0.7	0.7
Non-US	0.3	0.8	0.3	0.8
Global	8.7	10.3	8.7	10.3
Total Deposition (ug/m2)	13.4	28.8	11.3	16.0
Percent Reduction			15.5	44.5

References

Acosta-Ruiz, G. and B. Powers (2001): Preliminary Atmospheric Emissions Inventory of Mercury in Mexico. Source: http://www.epa.gov/ttnchie1/conference/ei12/mexico/acosta-ruiz.pdf.

Amyot, M., D.R.S. Lean, and G. Mierle (1997): Photochemical formation of volatile mercury in high arctic lakes. *Environ. Tox. and Chem.*, **16**, 2054–2063.

Appel, K.W., C. Chemel, S.J. Roselle, X.V. Francis, R.-M. Hu, R. S. Sokhi, S.T. Rao, S.Galmarini (2012): Examination of the Community Multiscale Air Quality (CMAQ) model performance over the North American and European domains. *Atmos. Environ.*, ***53***, *142-155.*

Bullock, O. R., and K. A. Brehme (2002): Atmospheric mercury simulation using the CMAQ model: formulation description and analysis of wet deposition results. *Atmos. Environ.*, ***36*(13)**, 2135−2146.

Bullock, O. R., Jr., D. Atkinson, T. Braverman, K. Civerolo, A. Dastoor, D. Davignon, J.-Y. Ku, K. Lohman, T.C. Myers, S. Seigneur, G. Sistla, K. Vijayaraghavan (2008): The North American Mercury Model Intercomparison Study (NAMMIS): Study description and model-to-model comparisons, *J. Geophys. Res.*, **113**, D17310, doi:10.1029/2008JD009803.

Bullock, O. R., Jr., et al. (2009), An analysis of simulated wet deposition of mercury from the North American Mercury Model Intercomparison Study, *J. Geophys. Res.*, **114**, D08301, doi:10.1029/2008JD011224.

Cave, M., S. Appana, M. Patel, K.C. Falkner, C.J. McCain, and G. Brock (2010): Polychlorinated biphenyls, lead and mercury are associated with liver disease in American adults: NHANES 2003-2004. Envin. Health. Persp., 118, 1735-1742.

Dudhia, J., 1989: Numerical study of convection observed during the Winter Monsoon Experiment using a mesoscale two–dimensional model. *J. Atmos. Sci.*, **46**, 3077–3107.

Dudhia, J, 1996: A multi-layer soil temperature model for MM5. Sixth Annual PSU/NCAR Mesoscale Model Users' Workshop, Boulder CO, July 1996, 49-50.

Engle, M.A., A. Kolker, D.E. Mose, J.A. East, J.A., and J.D. McCord (2008): Summary of Mercury and Trace Element Precipitation Results from the Culpeper, Virginia, Mercury Deposition Network Site (VA-08), 2002-2006: U.S. Geological Survey Open File Report 2008-1232, 31 p.,

Ericksen, J. A., Gustin, M. S., Xin, M., Weisberg, P. J., & Fernandez, G. C. J. (2006). Air–soil exchange of mercury from background soils in the United States. *Sci. Tot. Environ*., **366**, 851–863.

Fiore, A. M., D. J. Jacob, I. Bey, R. M. Yantosca, B. D. Field, and A. C. Fusco (2002), Background ozone over the United States in summer: Origin, trend, and contribution to pollution episodes, *J. Geophys. Res.*, **107(D15)**, 4275, doi:10.1029/2001JD000982.

Godowitch, J.M., R. C. Gilliam, and S. T. Rao (2011): Diagnostic Evaluation of Ozone Production and Horizontal Transport in a Regional Photochemical Air Quality Modeling System. *Atmos. Environ.*, **45(24)**:3977-3987.

Grigal, D.F. (2003): Mercury sequestration in forests and peatlands: a review. *J. of Environ. Qual.*, **32**, 393-405.

Hong, Song–You, Jimy Dudhia, and Shu–Hua Chen, 2004: A revised approach to ice microphysical processes for the bulk parameterization of clouds and precipitation. *Mon. Wea. Rev.*, **132**, 103–120.

Hong, S.–Y., and J.–O. J. Lim, 2006: The WRF single–moment 6–class microphysics scheme (WSM6). *J. Korean Meteor. Soc.*, **42**, 129–151.

Hong, Song–You, Yign Noh, Jimy Dudhia, 2006: A new vertical diffusion package with an explicit treatment of entrainment processes. *Mon. Wea. Rev.*, **134**, 2318–2341.

Kain, John S., 2004: The Kain–Fritsch convective parameterization: An update. *J. Appl. Meteor.*, **43**, 170–181.

Lahoutifard, N. M. Sparling, and D. Lean (2005): Total and methyl mercury patterns in Arctic snow during springtime in Resolute, Nanuvut, Canada. *Atmos. Environ.*, **39**, 7597-7606.

Li, Q. B., D.J. Jacob, I. Bey, P.I. Palmer, B.N. Duncan, B.D. Field, R.V. Martin, A.M. Fiore, R.M. Yantosca, D.D. Parrish, P.G. Simmonds, and S.J. Oltmans (2002): Transatlantic transport of pollution and its effects on surface ozone in Europe and North America, *J. Geophys. Res.*, **107(D13)**, 4166, doi:10.1029/2001JD001422.

LimnoTech (2013): Statewide Michigan Mercury TMDL. LimnoTech, Ann Arbor, MI.

Michigan Department of Environmental Quality (MDEQ) (2011): 2005 estimates of anthropogenic mercury air emissions in Michigan.

Mlawer, Eli. J., Steven. J. Taubman, Patrick. D. Brown, M. J. Iacono, and S. A. Clough (1997), Radiative transfer for inhomogeneous atmospheres: RRTM, a validated correlated–k model for the longwave. J. Geophys. Res., **102**, 16663–16682.

Monin A. S., and A. M. Obukhov, 1954: Basic laws of turbulent mixing in the surface layer of the atmosphere. Contrib Geophys Inst Acad Sci USSR **151**:163–187

Montiero, L.R., V. Costa., R.W. Furness, and R.S. Santos (1996): Mercury concentrations in prey fish indicate enhanced bioaccumulation in mesopelagic environments. *Mar. Ecol. Prog. Ser*, 141, 21-25.

Rowland, A.S., D.D. Baird, C.R. Weinberg, D.L. Shore, C.M. Shy and A.J. Wilcox (1994): The effect of occupational exposure to mercury vapour on the fertility of female dental assistants. *Occ. and Env. Med*., **51**, 28-24.

Sakamoto, M., A. Nakono and H, Akagi (2001): Declining Minimata birth ratio associated with increased male fetal death due to heavy methylmercury pollution. *Environ. Res.*, **87(2)**, 92-98.

Schroeder, W.H., Munthe, J. (1998): Atmospheric mercury—An overview. *Atmos. Environ*., **32**, No.5, 809-822.

Tewari, M., F. Chen, W. Wang, J. Dudhia, M. LeMone, K. Mitchell, M. Ek, G. Gayno, J. Wegiel, and R. Cuenca (2004): Implementation and verification of Unified Noah land surface model in the WRF model. Presented at the 84th AMS Conference, Seattle, WA, 11-15 January 2004.

Thompson, D.R., R.W. Furness, and L.R. Monteiro (1998): Seabirds as biomonitors of mercury inputs into epipelagic and mesopelagic marine food chains. *Sci. Tot. Environ*. , 213, 299-305.

U.S. Census Bureau (2005): U.S. Census Bureau, Estimated Population of Counties for April 2000 to July 2005. http://www.census.gov/popest/data/counties/totals/2005/CO-EST2005-01.html.

USEPA (2006a): Data Quality Assessment: A Reviewer's Guide (QA/G-9R**)** EPA/240/B-06/002 February 2006**.**

USEPA (2006b): Data Quality Assessment**:** Statistical Tools for Practitioners **(**QA/G-9S) EPA/240/B-06/003 February 2006**.**

Wang, Y., D. J. Jacob, and J. A. Logan, Global simulation of tropospheric ozone-NO_X-hydrocarbon chemistry, 3, Origin of tropospheric ozone and effects of non-methane hydrocarbons, *J. Geophys. Res.*, **103**, 10,757– 10,768, 1998.

Wiedinmyer, C. and H. Friedli (2007): Mercury emission estimates from fires: an initial inventory for the United States. *Environ. Sci. Technol.*, **41**, 8092–8098.

Wisconsin Department of Natural Resources (2006): Fate of mercury in products in Wisconsin. Flow model developed by Barr Engineering for Wisconsin Department of Natural Resources.

Yu, S., R. Mathur, G. Sarwar, D. Kank, D. Tong, G. Pouliot, AND J. E. Pleim (2010): Eta-CMAQ air quality forecasts for O3 and related species using three different photochemical mechanisms (CB4, CB05, SAPRC-99): Camparisons with measuremetns during the 2004 ICARTT Study. *Atmos. Chem and Phys.*, **10(6)**:3001-3025.

Zhang, H., S.E. Lindberg, F.J. Marsik and G.J. Keeler (2001): Mercury air/surface exchange kinetics of background soils of the Tahquamenon River watershed in the Michigan Upper Peninsula. *Water, Air and Soil Poll.*, **126**, 151-169.